DNA methylation and histone post-translational modifications in the mouse germline following in-vitro maturation of fresh or cryopreserved prepubertal testicular tissue

A. Oblette, J. Rondeaux, L. Dumont, M. Delessard, J. Saulnier, A. Rives, N. Rives, C. Rondanino

Running title: Epigenetic modifications in *in vitro* cultured mouse testes

Title: DNA methylation and histone post-translational modifications in the mouse germline following *in vitro* maturation of fresh or frozen/thawed prepubertal testicular tissue

Antoine Oblette*, Julie Rondeaux*, Ludovic Dumont, Marion Delessard, Justine Saulnier, Aurélie Rives, Nathalie Rives and Christine Rondanino

Normandie Univ, UNIROUEN, EA 4308 "Gametogenesis and Gamete Quality", Rouen University Hospital, Department of Reproductive Biology–CECOS, F 76000 Rouen, France
antoine.oblette1@univ-rouen.fr; julie.rondeaux@etu.univ-rouen.fr; ludovic.dumont1@univ-rouen.fr; marion.delessard@etu.univ-rouen.fr; justine.saulnier@etu.univ-rouen.fr; rivesaur@gmail.com; nathalie.rives@chu-rouen.fr; christine.rondanino@univ-rouen.fr

Corresponding author: Dr Christine Rondanino, Ph.D.; Phone: +33 2 35 14 82 94.

* The authors contributed equally to this work

Abstract

Research question: Do freezing/thawing and *in vitro* culture procedures affect the expression of DNA methyltransferases (DNMTs) and histone modifying enzymes, as well as the establishment of DNA methylation and histone post-translational modifications (PTMs) in germ cells in prepubertal mouse testicular tissue?

Design: We investigated the expression of epigenetic modification enzymes, DNA methylation and histone PTMs, and the spermatogenic progression after *in vitro* maturation of fresh or frozen/thawed mouse prepubertal testicular tissue. Fresh or thawed testicular fragments from 6-7 days *postpartum* mice were cultured for 30 days in the presence of retinol with or without follicle stimulating hormone (FSH).

Results: The *in vitro* maturation of fresh or frozen/thawed tissue allowed the differentiation of spermatogonia into spermatozoa. Differences in the levels of transcripts encoding epigenetic modifications enzymes (*Dnmt1, Dnmt3a*, *Prdm9*, *Jarid1b*, *Src1*, *Sirt1*, *Hdac1*) were found between 30-day tissue cultures and age-matched *in vivo* controls. DNMT1/DNMT3a expression and the presence of 5-methylcytosine (5mC) were detected in spermatogonia and leptotene/zygotene spermatocytes in cultures. The relative 5mC fluorescence intensity was similar in spermatozoa produced in cultures of frozen/thawed tissues or *in vivo*. H3K4me3, H3K9ac and H4K8ac were present in all germ cell types but differences in the proportion of germ cells containing these epigenetic marks were found after cultures.

Conclusions: Despite differences with the *in vivo* situation, DNA methylation and histone methylation and acetylation occur in the mouse germline in *in vitro* matured fresh or frozen/thawed mouse prepubertal testicular tissue, and the expression of the enzymes catalyzing these epigenetic modifications are maintained *in vitro*.

Keywords: mouse prepubertal testis, freezing protocols, *in vitro* spermatogenesis, epigenetic modification, DNA methylation, histone post-translational modifications.

Key message: In prepubertal boys with cancer, fertility preservation relies on testicular tissue freezing. *In vitro* maturation of frozen/thawed tissue is one of the approaches envisaged to restore fertility. The impact of the procedures on germline epigenetic modifications needs to be evaluated in an animal model before considering a human application.

Introduction

Survival rates for children with cancer have considerably increased over the past decades thanks to diagnostic and therapeutic progress. Treatments by chemotherapy and radiotherapy can however have toxic effects on gonads (Jahnukainen et al., 2015; Picton et al., 2015; Wyns et al., 2010). In prepubertal boys, the actively dividing spermatogonial stem cells (SSCs) are particularly sensitive to certain cytotoxic agents used in chemotherapy protocols (Goossens et al., 2013; Nurmio et al., 2009). At adulthood, cured patients can be diagnosed with a permanent infertility (oligozoospermia, azoospermia) with significant psychological consequences (Gies et al., 2015; Jahnukainen et al., 2015).

Because of the potential long-term sequelae of cancer treatment on reproductive functions, fertility preservation options have been developed and are proposed to patients prior to cancer therapy (Baert et al., 2012; Gies et al., 2015; Jahnukainen et al., 2015; Onofre et al., 2016; Picton et al., 2015; Wyns et al., 2015). For adolescents and adults, sperm can be cryopreserved before the beginning of gonadotoxic treatments and later used for assisted reproductive techniques. For prepubertal boys however, freezing the testicular tissue that contains SSCs is so far the only option. Freezing (slow freezing or vitrification) and thawing procedures have been optimized for immature testicular tissues in order to minimize ice crystal formation and cellular damage (Baert et al., 2012; Poels et al., 2013). We previously reported the development of optimal controlled slow freezing (CSF) and solid surface vitrification (SSV) protocols that preserve not only the architecture of mouse prepubertal tissue but also its exocrine and endocrine functions (Arkoun et al., 2016; Dumont et al., 2015; Milazzo et al., 2008).

In order to restore the fertility of cancer survivors who became sterile, thawed testicular tissues could theoretically be matured by *in vivo* or *in vitro* approaches to produce

spermatozoa for assisted reproduction (de Michele et al., 2017; Gies et al., 2015; Ibtisham et al., 2017; Yokonishi and Ogawa, 2016). The *in vivo* differentiation of SSCs could be achieved after autologous transplantation or autograft or eventually after xeno-transplantation or xenograft (Goossens et al., 2013; Milazzo et al., 2010; Poels et al., 2013). To avoid the potential reintroduction of malignant cells to surviving patients during auto-transplantation of cryopreserved testicular tissue or cells, especially to those treated for lymphoblastic acute leukemia, testicular tissues could be matured *in vitro* (Jahnukainen et al., 2015). Tridimensional and organotypic cultures are so far the only methods that allowed the production of spermatozoa from prepubertal murine testes (Abu Elhija et al., 2012; Arkoun et al., 2016; Dumont et al., 2015; Sato et al., 2011; Yokonishi et al., 2014). Notably, a complete *in vitro* spermatogenesis could be achieved in frozen (slow freezing or vitrification)/thawed mouse prepubertal testicular tissues cultured at a gas-liquid interphase (Arkoun et al., 2016; Dumont et al., 2015; Yokonishi et al., 2014). Our data moreover showed that supplementing the culture medium with 10^{-6} M retinol promoted SSCs differentiation and entry into meiosis as well as sperm production in fresh or frozen/thawed testes (Arkoun et al., 2015; Dumont et al., 2017, 2016; Rondanino et al., 2017). A recent study confirmed that retinoic acid and retinol play crucial roles in the onset of spermatogonial differentiation and meiotic initiation under organ culture conditions (Sanjo et al., 2018). The addition of follicle stimulating hormone (FSH), crucial for the initiation and progression of spermatogenesis, together with retinol in the medium had no additive effect on the spermatogenic yield (Arkoun et al., 2015). We recently reported that most of *in vitro* generated spermatozoa were haploid, contained unfragmented DNA and normally condensed chromatin like their *in vivo* counterparts (Oblette et al., 2017). Although the microinjection of *in vitro* produced spermatozoa into oocytes was capable of producing reproductively competent offspring (Sato et al., 2011; Yokonishi et al., 2014) with an almost normal state of methylation for 11 imprinted genes

(Yokonishi et al., 2014), the epigenetic modifications of germ cells in cultured prepubertal testes have never been studied. Epigenetic marks, including DNA methylation and histone post-translational modifications (PTMs), are however important during spermatogenesis for the proper maturation of gametes, and after fertilization the inherited marks play an essential role during embryonic development and can later influence offspring health and behavior (Champroux et al., 2018; Jenkins et al., 2017; Stewart et al., 2016; Stuppia et al., 2015; Yao et al., 2015; Boissonnas et al., 2013). DNA methylation is an epigenetic mechanism involving the covalent transfer of a methyl group onto the C5 position of cytosine to form the heritable mark 5-methylcytosine (5mC). This epigenetic modification, which is catalyzed by DNA methyltransferases (DNMT), represses the expression of numerous genes. DNMT1 is responsible for the maintenance of DNA methylation profiles during cell divisions (Uysal et al., 2016). DNMT3a and DNMT3b catalyze *de novo* DNA methylation in a heterodimer with the non-catalytic DNMT3L (Uysal et al., 2016). During mouse development, the genome of primordial germ cells undergoes a wave of demethylation between 8 and 13.5 days *post coïtum* (Boissonnas et al., 2013). *De novo* methylation marks are then established in a sex-specific manner. In males, *de novo* DNA methylation to establish paternally imprinted loci begins at around 15.5 days *post coïtum* and continues after birth in spermatogonia and spermatocytes. The process of *de novo* DNA methylation appears to be complete at the pachytene spermatocyte stage (Boissonnas et al., 2013; Yao et al., 2015). Knocking out the mouse *Dnmt1* gene was shown to induce embryonic lethality, and disruption of *Dnmt3a* and *Dnmt3l* genes led to impaired spermatogenesis (Jenkins and Carrell, 2012; Uysal et al., 2016). In men, abnormal sperm DNA methylation patterns have been associated with infertility, poor embryo quality and congenital diseases in the offspring (Cui et al., 2016; Gunes et al., 2016; Kitamura et al., 2015; McSwiggin and O'Doherty, 2018; Santi et al., 2017; Stuppia et al., 2015). Histone PTMs, such as methylation and acetylation, have been reported to be

126 associated with chromatin remodeling during spermatogenesis, including histone-to-
127 protamine replacement occurring within germ cells during spermiogenesis. Histone
128 methylation corresponds to the addition of one or several methyl groups on lysine (K) or
129 arginine (R) residues by histone methyltransferases (e.g. PRDM9) and can be reversed by
130 histone demethylases (e.g. JARID1B). PRDM9, which catalyzes the trimethylation of lysine 4
131 of histone H3 (H3K4me3), is essential for progression through early meiotic prophase,
132 including homologous chromosome pairing, DNA double-strand break repair and sex body
133 formation (Hayashi et al., 2005). This mark is associated with transcriptionally active genes
134 and is also enriched at developmental gene promoters within spermatozoa (Hammoud et al.,
135 2011). The acetylation of histones on lysine residues, an epigenetic modification found in
136 transcriptionally active chromatin regions, is catalyzed by histone acetyltransferases (e.g.
137 SRC1) and reversed by histone deacetylases (e.g. SIRT1, HDAC1). An increase in the
138 acetylation of histones H3 and H4 is observed in spermatogonia and spermatids compared to
139 spermatocytes (Boissonnas et al., 2013; Luense et al., 2016). The H3K9ac mark is essential
140 for the progression of spermiogenesis: alterations in H3K9ac levels induce morphological
141 abnormalities and apoptosis of round spermatids (Dai et al., 2015). Mice with a specific
142 deletion of *Sirt1* in male germ cells exhibit a defect in histone-to-protamine transition, altered
143 chromatin condensation, defects in acrosome biogenesis and decreased fecundity (Bell et al.,
144 2014; Liu et al., 2017). Moreover, a premature acetylation of histone H4 in spermatocytes or a
145 decrease of histone acetylation in spermatids have been reported in infertile men exhibiting
146 impaired spermatogenesis (Sonnack et al., 2002). Alterations in the genomic distribution of
147 the heritable marks H3K4me3, H3K9ac and H4K12ac have also been described in the
148 spermatozoa of infertile men (Hammoud et al., 2011; Steilmann et al., 2011; Vieweg et al.,
149 2015).

It has been demonstrated that DNMT1 and DNMT3A expression levels, DNA methylation status of germ cells and several histone PTMs (H3K4me3, H3K9ac, H4K12ac, H4K16ac) were unchanged after *in vivo* maturation of SSCs from prepubertal mouse testes by transplantation or graft (Goossens et al., 2011). However, H4K5ac and H4K8ac marks were altered after SSCs transplantation (Goossens et al., 2011). It appears therefore imperative to ascertain that DNA methylation and histone PTMs are not altered in the germline in organotypic cultures before applying *in vitro* maturation procedures to frozen/thawed testicular tissue from prepubescent boys. So far, the maintenance of DNA methylation has only been shown in 2 to 4-day cultures of rat fetal testes (Rwigemera et al., 2017) and in 7 to 21-day cultures of marmoset adult testes (Langenstroth-Röwer et al., 2017). Histone PTMs (H3K4me2, H3K4me3) were also maintained in short-term cultures (Rwigemera et al., 2017). In the present work, fresh, CSF or SSV mouse prepubertal testicular tissues were cultured for 30 days at a gas-liquid interphase in the presence of retinol alone or of a retinol/FSH alternation. The progression of *in vitro* spermatogenesis was analyzed. DNA methylation, active histone marks (H3K4me3, H3K9ac, H4K8ac) and the expression of catalytic DNMTs and histone modifying enzymes were studied in germ cells prior and following *in vitro* maturation.

Materials and Methods

Mice, testes collection and ethical approval

Prepubertal 6-7-day-old CD-1 male mice (Charles River Laboratories, L'Arbresle, France) were euthanized by decapitation. Testes were excised, rinsed and the tunica albuginea was removed in α-MEM at 4°C (Gibco by Life Technologies, Saint-Aubin, France). Testes were then divided in several batches and cultured either directly (culture of fresh tissues) or after

CSF or SSV and thawing (Additional File 1). In order to evaluate the impact of the freezing procedures on the testicular tissues before culture, fresh, CSF and SSV testes from mice aged 6-7 d*pp* were analyzed (Additional File 1). Moreover, mice aged 36-37 d*pp* were euthanized by CO_2 asphyxiation and their testes were used as *in vivo* controls for testes cultured *in vitro* for 30 days (Additional File 1). In total, 42 testes (14 fresh, 14 CSF, 14 SSV) from 21 mice aged 6-7 d*pp* were used for the analyses performed before culture, 72 testes (24 fresh, 24 CSF, 24 SSV) from 39 mice aged 6-7 d*pp* were used for *in vitro* maturation, and 20 testes from 13 mice aged 36-37 d*pp* were used as *in vivo* controls. A total of 134 testes from 73 mice were therefore used in this study (Additional File 1).

This study was conducted in accordance with the 3Rs principle. All the experimental procedures were approved by the Institutional Animal Care and Use Committee of Rouen University Hospital under the licence/protocol number N/23-11-12/46/11-15.

CSF and thawing of testicular tissues

Freezing procedure. Testes were frozen as previously described (Arkoun et al., 2016; Milazzo et al., 2008). Briefly, testes were incubated in cryotubes containing 1.3 mL of freezing medium: Leibovitz L-15 medium (Eurobio, Courtabœuf, France) supplemented with 1.5 M dimethylsulfoxyde (DMSO, Sigma-Aldrich, Saint-Quentin Fallavier, France), 0.05 M sucrose (Sigma-Aldrich) and 10% (v/v) fetal calf serum (FCS, Eurobio). Controlled slow freezing was performed in a programmable freezer (Nicool Freezal, Air Liquide, Marne-la-Vallée, France) with the following protocol: start at 5°C, then -2°C/minute until reaching -9°C, stabilization at -9°C for 7 minutes, then -0.3°C/minute until -40°C and -10°C/minute down to -140°C. The samples were then stored in liquid nitrogen.

Thawing procedure. Cryotubes were warmed for 1 minute at room temperature and then for 3 minutes at 30°C in a water bath. Testicular tissues were then successively incubated at 4°C in

baths containing decreasing concentrations of cryoprotective agents during 5 minutes each (*bath 1*: 1 M DMSO, 0.05 M sucrose, 10% FCS, Leibovitz L15; *bath 2*: 0.5 M DMSO, 0.05 M sucrose, 10% FCS, Leibovitz L15; *bath 3*: 0.05 M sucrose, 10% FCS, Leibovitz L15; *bath 4*: 10% FCS, Leibovitz L15).

SSV and thawing of testicular tissues

Vitrification procedure. Testes were vitrified as previously described (Dumont et al., 2015). Briefly, samples were incubated for 10 minutes at 4°C in Dulbecco's modified Eagle's medium/Nutrient Mixture F12 (DMEM/F12, Sigma-Aldrich) supplemented with 1.05 M DMSO and 1.35 M ethylene glycol (Sigma-Aldrich) and then for 5 minutes at 4°C in DMEM/F12 supplemented with 2.1 M DMSO, 2.7 M ethylene glycol, 0.5 M sucrose and 20% FCS. Testis samples were then dropped onto a thin aluminium floater (VWR, Fontenay-sous-Bois, France) partially immersed in liquid nitrogen. Vitrified testes were stored in cryotubes in liquid nitrogen.

Thawing procedure. Cryotubes were left at room temperature for 2 seconds. Testes were incubated in DMEM/F12 supplemented with 0.5 M sucrose and 20 % FCS for 2 minutes at 37°C, and then in DMEM/F12 supplemented with 20 % FCS for 2 minutes at 37°C. They were then successively transferred into four baths of DMEM/F12 supplemented with 20 % FCS for 5 minutes at 4°C.

Organotypic cultures

In vitro tissue cultures were performed at a gas-liquid interphase as previously described (Arkoun et al., 2016; Dumont et al., 2015; Sato et al., 2011; Yokonishi et al., 2014). Briefly, fresh or frozen/thawed testes were first cut into 4 fragments. They were placed on the top of two 1.5% (w/v) agarose Type I low EEO gels (Sigma-Aldrich) half-soaked in base medium

containing α-MEM, 10% KnockOut Serum Replacement (KSR, Gibco by Life Technologies) and 5 µg/mL gentamicin (Sigma-Aldrich). Testicular tissues were then cultured in 6-well plates (Dominique Dutscher, Brumath, France) under 5% CO_2 at 34°C for 30 days (D30), which corresponds to the end of the first spermatogenic wave. In the Rol condition, testicular fragments were cultured with base medium supplemented with 10^{-6} M retinol (Sigma-Aldrich). In the Rol/FSH condition, testicular samples were alternatively cultured with base medium containing 10^{-6} M retinol or 500 UI/L recombinant FSH (Gonal-f, Merck Serono, Lyon, France), with retinol being added every 8 days to coincide with the entry of spermatogonia into meiosis. In total, 288 testicular fragments from 72 testes were *in vitro* cultured and analyzed. RT-qPCR analyses were repeated 3 times (from 3 different testes) for *Dnmt1* and *Dnmt3a*, and 3 times for *Prdm9*, *Jarid1b*, *Src1*, *Sirt1* and *Hdac1*. Immunohistochemical analyses were repeated 4 times (from 4 different testes) for DNMT1, DNMT3a and 5mC, and 4 times for H3K4me3, H3K9ac and H4K8ac.

RNA extraction, reverse transcription and qPCR

RNA extraction. Total RNA was extracted from testicular samples (around 2 mg) using RNeasy Micro kit (Qiagen, Courtabœuf, France) according to the manufacturer's instructions. To remove contamination with genomic DNA, RNA was incubated with 2 units of TURBO DNase (Life Technologies) for 45 minutes at 37°C.

Reverse transcription. cDNA synthesis was performed using qScript cDNA SuperMix (Quanta Biosciences by VWR) according to the manufacturer's instructions using the following program: 5 minutes at 25°C, 30 minutes at 42°C and 5 minutes at 85°C.

qPCR. cDNA amplifications were carried out in a total volume of 20 µL containing 2 µL of cDNA templates diluted 1:10 (10 ng) in sterile water, 10 µL of Fast SYBR Green Master Mix (Applied Biosystems, Saint-Aubin, France) and 300 nM of each primer. Specific primers are

listed in Additional File 2. Reactions were performed in 96-well plates (Invitrogen by Life Technologies) in a StepOnePlus thermocycler (Applied Biosystems). Annealing temperatures were optimized for all primer sets (Additional File 2) and the efficiency of the reactions was determined using serial dilutions of cDNA samples. The amplification condition was 20 seconds at 95°C followed by 40 cycles (3 seconds at 95°C, 30 seconds at the annealing temperature). Melting curves were also obtained to ensure the specificity of PCR amplifications. The size of the amplicons was verified by agarose gel electrophoresis (E-gel 4%, Life Technologies). The relative expression level of each gene (*Dnmt1*, *Dnmt3a*, *Prdm9*, *Jarid1b*, *Src1*, *Sirt1* and *Hdac1*) was normalized to the housekeeping gene *Gapdh*. Data were analyzed using the $2^{-\Delta\Delta Ct}$ method.

Histological analyses

Tissue fixation and processing. Testicular tissues were fixed with Bouin's solution (Sigma-Aldrich) for 2 hours at room temperature. They were then dehydrated in ethanol in the Citadel 2000 tissue processor (Shandon, Cheshire, UK) and embedded in paraffin.

Tissue sectioning. Tissue sections (3 µm thick) were performed with the JungRM 2035 microtome (Leica) and were mounted on Polysine slides (Thermo Fisher Scientific, Waltham, MA, USA).

Immunohistochemical staining. Tissue sections were deparaffinized in two baths of xylene for 5 minutes and rehydrated in decreasing concentrations of ethanol. After a 5-minute wash in Tris buffer containing 10% Tween-20 (TBST, Microm Microtech, Francheville, France), sections were incubated for 40 minutes at 96°C in 10 mM citrate buffer (pH 6.0) and then cooled for 20 minutes at room temperature. Endogenous peroxidases were blocked with HP Block (Dako, Les Ulis, France) for 5 minutes at room temperature. Sections were washed for 5 minutes in distilled water and blocked with Ultra-V blocking solution (Thermo Fisher

Scientific) for 10 minutes at room temperature. They were then incubated overnight at 4°C with primary antibodies: rabbit polyclonal anti-DNMT1 IgGs (1:100 for 36-37 d*pp in vivo* testes and 30-day cultures of testicular tissues, 1:200 for 6-7 d*pp* testes, ab19905, Abcam, Paris, France), rabbit polyclonal anti-DNMT3a IgGs (1:1250, SC-20703, SantaCruz Biotechnology, Heidelberg, Germany), mouse monoclonal anti-5mC IgGs (1:50, 16233D3, Merck Millipore, Fontenay-sous-Bois, France), rabbit polyclonal anti-H3K4me3 IgGs (1:200 for 36-37 d*pp in vivo* testes and 30-day cultures of testicular tissues, 1:500 for 6-7 d*pp* testes, ab8580, Abcam), rabbit polyclonal anti-H3K9ac IgGs (1:50, ab61231, Abcam) or rabbit polyclonal anti-H4K8ac IgGs (1:1500 for 36-37 d*pp in vivo* testes and 30-day cultures of testicular tissues, 1:2000 for 6-7 d*pp* testes, ab15823, Abcam). After a 5-minute wash in TBST, biotinylated goat anti-rabbit antibodies (1:200, Santa Cruz, 25 minutes for DNMT1, DNMT3a and H3K9ac; undiluted, Thermo Fisher Scientific, 5 minutes for H3K4me3 and H4K8ac) or anti-mouse antibodies (Thermo Fisher Scientific, for 5mC) were applied at room temperature. The immunoreaction was visualized after incubation with horseradish peroxidase-conjugated streptavidin (Thermo Fisher Scientific) for 5 minutes at room temperature followed by the addition of 3,3'-diaminobenzidine (Thermo Fischer Scientific) for around 10 seconds (DNMT1 and H3K9ac), 20 seconds (DNMT3a), 30 seconds (H3K4me3) or 40 seconds (5mC and H4K8ac). Sections were finally counterstained with hematoxylin (Dako) for 15 seconds and mounted with Eukitt (CML, Nemours, France). Immunostaining with pre-immune rabbit IgGs (SC-2027, SantaCruz Biotechnology) or mouse IgGs (SC-2025, SantaCruz Biotechnology) was used as a negative control. Images were acquired at a ×500 magnification on a DM4000B light microscope (Leica, Solms, Germany) equipped with the Leica Application Suite Core v2.4 Software.

In each testicular sample analyzed, the expression and localization of DNMT1 and DNMT3a, the presence of 5mC residues and modified histones (H3K4me3, H3K9ac and H4K8ac) and

the number of each cell type (Sertoli cells: irregular nuclei, spermatogonia: smooth spherical nuclei close to the basal membrane, leptotene/zygotene spermatocytes: irregular spherical nuclei with condensed chromatin, pachytene spermatocytes: irregular spherical nuclei with highly condensed chromatin, round spermatids: small and regular round nuclei, elongated spermatids: elongated nuclei with highly condensed chromatin) per seminiferous tubule were analyzed in 30 cross-sectioned seminiferous tubules from 3 different sections. For *in vivo* controls, the 30 seminiferous tubules were examined in multiple microscopic fields chosen at random. However, almost all seminiferous tubules present in *in vitro* matured testes were analyzed because of the small size of the testicular fragments. The percentage of each germ cell type that stained positive for DNMT1, DNMT3a, 5mC, H3K4me3, H3K9ac and H4K8ac was calculated in each seminiferous tubule.

Sperm DNA methylation

Testicular sperm extraction. Testicular spermatozoa were extracted from a pool of 6 testes (from 6 different mice) for each condition. Briefly, tissues were placed in α-MEM pre-warmed at 37°C. After the careful removal of the central necrotic area using 27-gauge needles, tissues were mechanically dispersed. After a 10-minute centrifugation at 300 × *g*, pellets containing testicular cells were recovered. Cells were fixed with methanol for 30 minutes at -20°C and then spread onto glass slides.

Immunofluorescent staining of 5mC. After 5 minutes in TBST at room temperature, cells were permeabilized in acetone for 2 minutes. Nuclei were decondensed with 1 M NaOH for 4 minutes and in TBST containing 10 mM dithiothreitol and 0.1% (v/v) Triton X-100 (Sigma-Aldrich) for 20 minutes at 4°C. Slides were washed twice in TBST for 5 minutes and non-specific binding sites were blocked with 5% (w/v) horse serum albumin in TBST (Sigma-Aldrich). They were then incubated overnight at 4°C with mouse monoclonal anti-5mC IgGs

(1:50, 16233D3, Merck Millipore). After two washes in TBST for 5 minutes, Alexa Fluor 488 conjugated-goat anti-mouse IgGs (1:200, ab150113, Abcam) were applied for 1 hour at room temperature. After a 10-minute wash, cells were counterstained with 4',6-diamidino-2-phenylindole (DAPI, Counterstain I, 30-804931, Adgenix, Voisins-Le-Bretonneux, France). A negative control was carried out by omitting the primary antibody. Images were captured at a ×900 magnification by a U-CMAD3 camera mounted on a BX61 epifluorescence microscope (Olympus), with a fixed acquisition and exposure for each condition. Image acquisitions were carried out using the Bioview 234 Duet v2.3 image analyzer (Nes Ziona, Israël).

Fluorescence intensity quantification. For each experimental condition, a hundred spermatozoa (from a pool of 6 different *in vitro* cultured testes or from 6 *in vivo* testes), identified by their hook-shaped heads, was examined. The border around the sperm nuclei was manually delineated according to DNA staining. After subtracting the background, 5mC and DAPI fluorescence intensities were calculated for each spermatozoon using the ImageJ v1.8 software (National Institute of Health, Bethesda, MD, USA). For each sperm nucleus, the fluorescence of 5mC was divided by the fluorescence of DAPI to obtain normalized 5mC fluorescence.

Statistical analyses

Statistical analyses were carried out with the statistical GraphPad Prism 6 software (GraphPad Software Inc., La Jolla, CA, USA). To evaluate the impact of the freezing procedure on testicular tissue, data obtained from fresh 6-7 d*pp* testes were compared with those obtained from CSF or SSV 6-7 d*pp* testes using the non-parametric Kruskal Wallis test followed by the Dunn *post hoc* test. Data from 36-37 d*pp* testes and from 30-day cultured tissues, as well as data from cultures of fresh, CSF and SSV testicular tissues were also compared using the non-

parametric Kruskal Wallis test followed by the Dunn *post hoc* test. Cultures performed under the Rol or Rol/FSH conditions were compared using the non-parametric Mann Whitney test. Finally, the normalized 5mC fluorescence intensities were compared using the non-parametric Mann Whitney test. Data are expressed as mean ± SD. For each test, a value of $P < 0.05$ (*) or $P < 0.01$ (**) was considered statistically significant.

Results

DNA methylation and histone PTMs in fresh or frozen/thawed prepubertal mouse testicular tissue

To determine whether the transcripts encoding epigenetic modification enzymes are present in 6-7 days *postpartum* (d*pp*) testes and whether their levels are altered by a freezing/thawing cycle, qPCR analyses were performed on fresh, CSF or SSV testicular tissues. *Dnmt1* and *Dnmt3a* transcripts encoding catalytic DNMTs, *Prdm9* and *Jarid1b* transcripts encoding a histone methyltransferase and demethylase respectively, *Src1* transcripts encoding a histone acetyltransferase, and *Sirt1* and *Hdac1* transcripts encoding histone deacetylases were detected at 6-7 d*pp* (Figure 1A,B). Moreover, mRNA levels were not significantly different between fresh and frozen/thawed testes, regardless of the freezing/thawing protocol used, except for lower *Hdac1* mRNA levels in SSV *versus* fresh and CSF testes (Figure 1A,B). The expression of the catalytic DNMTs and the presence of the epigenetic marks 5mC, H3K4me3, H3K9ac and H4K8ac were then studied in prepubertal testes by immunohistochemistry (Figure 1C). At 6-7 d*pp*, seminiferous tubules only contained Sertoli cells and spermatogonia. DNMT1 and 5mC were detected in a majority of spermatogonia, and no significant difference was observed between fresh, CSF and SSV testes (Figure 1D). In contrast, spermatogonia did not express DNMT3a in fresh tissues while around 24% of

spermatogonia expressed this enzyme in CSF tissues ($P < 0.05$, Figure 1D). The three modified histones were found in a minority of spermatogonia in both fresh and frozen/thawed testes (Figure 1E).

Advancement of spermatogenesis in 30-day *in vitro* cultures of 6-7 d*pp* testicular tissues

As previously described (Arkoun et al., 2016, 2015; Dumont et al., 2017, 2016; Rondanino et al., 2017), a complete spermatogenesis can be achieved *in vitro* within fresh, CSF and SSV prepubertal testicular tissues after 30 days of culture in the presence of 10^{-6} M retinol (Rol culture condition). Indeed, germ cells at all stages of differentiation were found after organotypic cultures (Table 1). In an effort to further increase the yield of *in vitro* produced spermatozoa, the supplementation of culture medium with FSH in alternation with retinol (Rol/FSH culture condition) was tested in this study. The progression of spermatogenesis in cultures of fresh, CSF and SSV tissues cultured with Rol or Rol/FSH was evaluated and compared by determining the proportion of the different germ cell types per seminiferous tubule as well as the proportion of seminiferous tubules at the most advanced stage of differentiation.

We first compared the progression of spermatogenesis in 30-day cultures of fresh tissues and in the 36-37 d*pp* age-matched *in vivo* controls. The proportion of pachytene spermatocytes and of round and elongated spermatids per tubule were lower in cultures of fresh tissues than *in vivo* (Table 1). The proportion of tubules having reached the pachytene spermatocyte and the round spermatid stages was higher in cultures of fresh tissues than in controls (Table 2). In contrast, the percentage of tubules with elongated spermatids as the most advanced stage was significantly reduced in cultures of fresh tissues compared to *in vivo* (Table 2).

The impact of the freezing/thawing procedures on the advancement of spermatogenesis was then investigated. The different germ cell types were also present in CSF and SSV tissues

following *in vitro* maturation with Rol or Rol/FSH (Table 1). The proportion of pachytene spermatocytes per tubule was similar between cultures of fresh, CSF and SSV tissues in the presence of Rol. With Rol/FSH however, the percentage of pachytene spermatocytes per tubule was higher in cultures of frozen/thawed tissues than in fresh tissues (Table 1). The proportion of round and elongated spermatids per tubule was lower in cultures of CSF tissues than in fresh tissues, whatever the medium used (Table 1). This diminution was not observed in SSV tissues. The proportion of elongated spermatids per seminiferous tubule was even more elevated in cultures of SSV tissues with Rol/FSH than in cultures of CSF tissues (Table 1). The percentage of tubules with pachytene spermatocytes as the most advanced type of germ cells was more elevated in CSF tissues matured in the presence of Rol or Rol/FSH and in SSV tissues matured in the presence of Rol/FSH than in fresh tissues (Table 2). The percentage of seminiferous tubules in which round spermatids are the most differentiated germ cells were almost similar in cultures of fresh, CSF and SSV tissues. Indeed, their proportion was only lower in cultures of SSV tissues with Rol/FSH (Table 2). At last, fewer tubules reached the elongated spermatid stage in CSF tissues cultured with Rol or Rol/FSH and in SSV tissues cultured with Rol than in fresh tissues (Table 2).

The Rol and Rol/FSH culture conditions were finally compared. The proportion of Sertoli cells, spermatogonia, pachytene spermatocytes and round spermatids per tubule was not significantly different when FSH was added in cultures of fresh or frozen/thawed tissues (Table 1). In addition, the proportion of elongated spermatids per tubule was reduced in cultures of fresh and CSF tissues with Rol/FSH (Table 1). The percentage of tubules in which pachytene spermatocytes are the most differentiated germ cells were more elevated in fresh or SSV tissues cultured with Rol/FSH than with Rol alone (Table 2). Moreover, the percentage of tubules reaching the round spermatid stage was diminished in SSV tissues cultured with Rol/FSH (Table 2). The proportion of tubules containing elongated spermatids was higher

when fresh or CSF tissues were cultured with Rol than with Rol/FSH (Table 2). This parameter was however not influenced by the medium composition in cultures of SSV tissues.

DNA methylation and histone PTMs in 30-day *in vitro* cultures of fresh 6-7 d*pp* testicular tissues

Since the best spermatogenic progression was obtained in tissues cultured with Rol, this culture condition was selected for the rest of the study. The impact of organotypic culture and freezing procedures on the expression of epigenetic modification enzymes, on DNA methylation and histone PTMs was evaluated in *in vitro* matured testicular tissues.

Transcript levels were quantified by qPCR in fresh 6-7 d*pp* testicular tissues cultured *in vitro* for 30 days and compared with those measured in control 36-37 d*pp* testes. No significant difference in *Dnmt1* and *Dnmt3a* mRNA levels was found in tissues matured *in vitro* with Rol and *in vivo* controls (Figure 2A). While the levels of *Prdm9* and *Jarid1b* transcripts were similar in cultures of fresh tissues and in controls, *Src1*, *Sirt1* and *Hdac1* mRNA levels were lower *in vitro* (Figure 2B).

The expression of the DNMT1 and DNMT3a proteins, DNA methylation onto the C5 position of cytosines and the presence of the three active histone marks were detected in a majority of spermatogonia and leptotene/zygotene spermatocytes in 36-37 d*pp* testes (Figures 3 and 4). Moreover, more than half of round spermatids contained H3K4me3 and H3K9ac at 36-37 d*pp* while H4K8ac was found in a lesser proportion of these cells (Figure 4). The percentage of spermatogonia expressing DNMT1 and DNMT3a was similar in fresh tissues cultured with Rol and *in vivo* (Figure 3B). The proportion of leptotene/zygotene spermatocytes expressing DNMT1 in cultures of fresh tissues was also comparable to *in vivo* controls (Figure 3B). In contrast, a lower percentage of spermatocytes expressing DNMT3a was noticed in tissues cultured with Rol (Figure 3B). The percentage of spermatogonia with methylated DNA was

reduced in fresh tissues cultured with Rol compared to 36-37 d*pp* control testes (Figure 3B). However, the proportion of leptotene/zygotene spermatocytes with 5mC labelling was not significantly different in fresh tissue cultures and *in vivo* (Figure 3B). DNMT1, DNMT3a and 5mC labelling in pachytene spermatocytes, round and elongated spermatids were exceptionally observed in both 36-37 d*pp* controls and 30-day cultures of 6-7 d*pp* testicular tissues. A lower proportion of spermatogonia, round and elongated spermatids containing H3K4me3 was found in cultures of fresh tissues than *in vivo* ($P < 0.05$, Figure 4B). The percentage of spermatogonia ($P < 0.05$), round and elongated spermatids ($P < 0.01$ and $P < 0.05$ respectively) containing H3K9ac was also diminished in organotypic cultures (Figure 4C). Finally, H4K8ac was found in less spermatogonia and leptotene/zygotene sperrmatocytes in *in vitro* matured fresh tissues ($P < 0.05$, Figure 4D).

Epigenetic modifications in 30-day *in vitro* cultures of CSF or SSV 6-7 d*pp* testicular tissues

To determine whether the freezing and thawing of 6-7 d*pp* testicular tissues could influence the expression of genes encoding epigenetic modification enzymes in 30-day organotypic cultures, qPCR analyses were performed on *in vitro* matured CSF or SSV tissues and compared with the data obtained from fresh tissue cultures. Apart from 7.6-fold lower *Dnmt1* mRNA levels in SSV tissues cultured with Rol ($P < 0.05$, Figure 2A), *Dnmt1* transcript levels did not vary in a significant manner in cultures of CSF tissues with Rol compared to cultures of fresh tissues (Figure 2A). Furthermore, no significant difference in *Dnmt3a* transcript levels was found after culture of fresh or frozen/thawed testicular tissues (Figure 2A). Moreover, apart from 3.9-fold higher *Hdac1* mRNA levels in cultures of SSV tissues, the levels of the transcripts encoding histone modifying enzymes were not significantly different between cultures of fresh, CSF and SSV tissues (Figure 2B). However, lower *Dnmt3a* and

475 *Hdac1* mRNA levels were found in cultures of CSF tissues and lower *Dnmt1*, *Dnmt3a* and
476 *Jarid1b* mRNA levels were found in cultures of SSV tissues compared to *in vivo* controls
477 (Figure 2).
478 DNMT1, DNMT3a, 5mC, H3K4me3, H3K9ac and H4K8ac labelling in CSF or SSV tissue
479 cultures were compared to those observed in fresh tissue cultures (Figures 5 and 6). DNMT1,
480 DNMT3a and the 5mC epigenetic mark were found in a majority of spermatogonia in cultures
481 of fresh, CSF or SSV tissues (Figure 5B). Most of the leptotene/zygotene spermatocytes
482 found in cultures of fresh or frozen/thawed tissues expressed DNMT1 and contained 5mC
483 residues (Figure 5B). The proportion of leptotene/zygotene spermatocytes expressing
484 DNMT3a did not appear to be different among those under fresh, CSF, or SSV conditions
485 (Figure 5B). As in the case of fresh tissue cultures, DNMT1, DNMT3a and 5mC were rarely
486 detected in pachytene spermatocytes, round and elongated spermatids. The proportion of
487 elongated spermatids containing H3K4me3 was higher in cultures of CSF and SSV tissues
488 than in fresh tissues (Figure 6B). The proportion of spermatogonia and elongated spermatids
489 containing H3K9ac were more elevated in cultures of CSF tissues than in fresh tissues (Figure
490 6C). This epigenetic mark was also present in a higher proportion of spermatogonia, round
491 and elongated spermatids in cultures of SSV tissues compared to fresh tissues (Figure 6C).
492 Finally, a lower proportion of round spermatids contained H4K8ac in cultures of CSF tissues
493 and the percentage of H4K8ac-postive pachytene spermatocytes was lower in cultures of CSF
494 and SSV tissues than in fresh tissues (Figure 6D).
495
496 **DNA methylation in spermatozoa extracted from 30-day *in vitro* cultures of fresh, CSF**
497 **or SSV 6-7 d*pp* testicular tissues**
498 Despite our attempts using various antigen retrieval procedures, 5mC labelling was rarely
499 detected in germ cells beyond the leptotene/zygotene stage in both *in vivo* controls and *in*

vitro matured testicular tissues. In order to ascertain that the genome of *in vitro* produced gametes was methylated, spermatozoa were extracted from cultures of fresh, CSF or SSV tissues, their nuclei were decondensed and the presence of the heritable 5mC epigenetic mark was investigated by immunofluorescence (Figure 7). The presence of methylated cytosines was detected in the nuclei of spermatozoa. The expression of 5mC between sperm nuclei was heterogeneous. Specifically, the normalized 5mC fluorescence intensity ranged from 0.01 to 0.85 (median = 0.16) in spermatozoa extracted from 36-37 d*pp* testes (Figure 7B). Similar 5mC levels were found in spermatozoa produced in cultures of CSF or SSV tissues (median = 0.14 and 0.10, respectively), but lower levels were noticed in spermatozoa generated in cultures of fresh tissues (median = 0.10) (Figure 7B). Because of the low spermatogenic yield in cultures, our repeated attempts to analyze the methylation patterns of two imprinted genes (*H19* and *Igf2r*) in extracted spermatozoa by bisulfite pyrosequencing were unsuccessful.

Discussion

In the present study, no major alterations of the expression of DNMT1 and DNMT3a, two essential catalytic DNA methyltransferases, and of DNA methylation was found in germ cells after *in vitro* maturation of fresh or frozen/thawed mouse prepubertal testes, when compared to those allowed to develop *in vivo*. However, differences in the levels of transcripts encoding histone modifying enzymes and in the distribution of the H3K4me3, H3K9ac and H4K8ac marks were found between *in vitro* and *in vivo* matured testes.

The fertility of childhood cancer survivors could be restored by producing spermatozoa from SSCs with *in vivo* or *in vitro* approaches (de Michele et al., 2017; Gies et al., 2015; Ibtisham et al., 2017; Yokonishi and Ogawa, 2016). It has been previously demonstrated that mouse germ cells from fresh prepubertal testes go through typical DNA methylation after SSCs

525 transplantation and testicular tissue grafting, and that germ cells present alteration in H4K5ac
526 and H4K8ac marks after SSCs transplantation but not after tissue grafting (Goossens et al.,
527 2011). If the methylation status of 11 imprinted genes is almost normal in the offspring
528 derived from *in vitro* produced spermatozoa, the examination of DNA methylation in germ
529 cells following organotypic culture is warranted, as previously highlighted (Yokonishi et al.,
530 2014). Moreover, histone PTMs have never been investigated in *in vitro* matured prepubertal
531 testicular tissues.
532 Fresh or frozen (by CSF or SSV)/thawed 6-7 d*pp* testicular tissues were first analyzed in this
533 study. *Dnmt1* and *Dnmt3a* gene expression was detected in these testes, which is in
534 accordance with previous data showing that transcripts were present postnatally (La Salle et
535 al., 2004; La Salle and Trasler, 2006; Mertineit et al., 1998). Here, no significant differences
536 in *Dnmt1* or *Dnmt3a* mRNA levels were observed among fresh, CSF and SSV tissues. As
537 previously reported (La Salle et al., 2004; Mertineit et al., 1998), we detected the DNMT1
538 protein in spermatogonia in postnatal testes. In contrast, this enzyme was not found in the
539 mouse prepubertal testis in another study (Goossens et al., 2011). Since the age of the mice
540 was not specified, this discrepancy might come from the analysis of testes at different
541 developmental stages. We observed that spermatogonia present in fresh 6-7 d*pp* testes
542 contained the 5mC epigenetic mark but did not express DNMT3a. This is consistent with a
543 previous report showing that DNMT3a was only detected in Sertoli and myoid cells while
544 5mC was present in spermatogonia (Goossens et al., 2011). The presence of methylated
545 cytosines in spermatogonia indicates that methylation profiles were, at least in part,
546 established at this stage. Indeed, following a demethylation wave during embryonic
547 development, spermatogonial precursor cells and spermatogonia then undergo *de novo* DNA
548 methylation (Boissonnas et al., 2013; Kubo et al., 2015; Yao et al., 2015). While the presence
549 of DNMT1 suggests that DNA methylation profiles are maintained during SSC division, the

lack of DNMT3a may however mean that *de novo* methylation is not occurring in spermatogonia at 6-7 d*pp*. In the present study, DNMT1 expression and 5mC marks were also observed in spermatogonia of thawed CSF or SSV testes. For unknown reasons and contrary to fresh tissues, DNMT3a was found in spermatogonia in frozen/thawed tissues, and may cause in these cells the appearance of abnormal DNA methylation profiles and the repression of gene expression. Moreover, we showed that the *Prdm9*, *Jarid1b*, *Src1*, *Sirt1* and *Hdac1* genes encoding histone modifying enzymes were expressed in fresh, CSF and SSV 6-7 d*pp* testes. In contrast to a previous study (Goossens et al., 2011), we detected the H3K9ac mark not only in Sertoli cells but also in a small fraction of spermatogonia. The H3K4me3 and H4K8ac marks were also present in these two cell types, as previously described (Goossens et al., 2011).

Before analyzing DNA methylation and histone PTMs in *in vitro* matured prepubertal testicular tissues, the advancement of spermatogenesis was examined. As previously shown (Arkoun et al., 2016, 2015; Dumont et al., 2016, 2015; Sato et al., 2011; Yokonishi et al., 2014), a successful differentiation of spermatogonia into spermatozoa was obtained in the present study after culture of fresh or frozen/thawed prepubertal testicular tissues at a gas-liquid interphase. The proportion of elongated spermatids per seminiferous tubule and of tubules having reached the elongated spermatid stage were lower in 30-day cultures of fresh tissues compared to *in vivo* controls. Moreover, these parameters were reduced in CSF tissues compared to fresh or SSV tissues. Our data therefore suggest that vitrification better preserves testicular tissues than slow freezing, and are in line with our previous data reporting better spermatogenic yields in cultures of SSV than CSF tissues (Dumont et al., 2015). To promote germ cell differentiation, tissues were cultured with retinol alone or with an alternation retinol/FSH. Indeed, probably because of the complex interactions between retinoids and FSH (Livera et al., 2002), no additive effect has been previously observed on *in vitro*

spermatogenesis when retinol and FSH were combined together (Arkoun et al., 2015). We found that the proportion of elongated spermatids per tubule and of tubules containing elongated spermatids was significantly reduced in fresh and CSF tissues cultured with retinol/FSH rather than retinol alone. In order to mimic *in vivo* conditions as closely as possible, different concentrations of FSH (corresponding to the physiological variations of this hormone) will have to be used during the course of *in vitro* cultures in future studies. Moreover, the culture medium will have to be supplemented with other factors that positively influence spermatogenesis. Indeed, recently, the use of a chemically-defined medium containing retinoic acid, retinol and a combination of four hormones (FSH, LH, testosterone, triiodothyronine) was found to promote spermatogenesis until round spermatid production (Sanjo et al., 2018).

In this study, *Dnmt1* and *Dnmt3a* transcripts were detected *in vivo* at 36-37 d*pp* and in fresh, CSF and SSV tissues cultured for 30 days. Differences in their levels were evidenced between *in vivo* controls and cultures of fresh or frozen/thawed tissues. DNMT1, DNMT3a and 5mC residues were mostly localized in spermatogonia and leptotene/zygotene spermatocytes *in vivo* and in cultures of fresh or frozen/thawed tissues. The presence of DNMT1 and DNMT3a specifically in spermatogonia and leptotene/zygotene spermatocytes during spermatogenesis is in agreement with previous studies (La Salle and Trasler, 2006; Mertineit et al., 1998; Watanabe et al., 2004). In adult testis, DNMT1 has also been detected in pachytene spermatocytes, diplotene spermatocytes, round spermatids and 5mC was also found in round spermatids (Goossens et al., 2011). The expression of DNMT3a in 36-37 d*pp* testes and 30-day cultures suggests that *de novo* methylation is occurring at this stage. Here, the epigenetic 5mC mark was not found in germ cells beyond the leptotene/zygotene spermatocyte stage *in vivo* and in organotypic cultures. As suggested previously (Goossens et al., 2011), the lack of 5mC staining in pachytene spermatocytes could be due to the fact that the methylation pattern

has not yet been set on daughter DNA strand. The lack of labelling in spermatids may however be explained by a poor accessibility of antibodies to the condensed DNA. To ascertain that DNA methylation marks are indeed found in most differentiated germ cells, we extracted spermatozoa from the testicular tissues after culture and performed 5mC labelling on decondensed DNA. The epigenetic mark 5mC was detected in the nuclei of spermatozoa generated in cultures of fresh or frozen/thawed testicular tissues. The relative 5mC fluorescence intensity was similar in spermatozoa produced in cultures of frozen/thawed tissues or *in vivo*, but was lower in spermatozoa extracted from cultures of fresh tissues. It has been shown that the DNA methylation patterns of a paternally methylated gene (*Igf2*) and a maternally expressed gene (*Peg1*) in epididymal spermatozoa obtained after SSC transplantation were not different from controls (Goossens et al., 2009). In our study, the analysis of the methylation status of the paternally imprinted gene *H19* and the maternally imprinted gene *Igf2r* in *in vitro* produced spermatozoa could not be achieved. Indeed, a heterogeneous cell population, among which few spermatozoa, was obtained after mechanical dissociation of *in vitro* matured testes.

In addition, our data showed that *Prdm9*, *Jarid1b*, *Src1*, *Sirt1* and *Hdac1* transcripts were also present in 36-37 d*pp* testes and in fresh or frozen/thawed tissues cultured for 30 days. The levels of *Src1*, *Sirt1* and *Hdac1* mRNA encoding histone acetyltransferase or deacetylase were lower in cultures of fresh tissues than *in vivo*. However, apart from lower mRNA levels of *Jarid1b* in cultures of SSV tissues and of *Hdac1* in cultures of CSF tissues, the levels of transcripts encoding the different histone modifying enzymes were similar between cultures of frozen/thawed tissues and *in vivo*. As previously reported (Godmann et al., 2007; Goossens et al., 2011; Hazzouri et al., 2000; Zhang et al., 2014), we found that H3K4me3, H3K9ac and H4K8ac were present in spermatogonia, leptotene/zygotene spermatocytes, round and elongated spermatids and in few pachytene spermatocytes *in vivo*. An altered distribution of

these three active histone marks was observed in our organotypic cultures. We observed that the H3K4me3 and H3K9ac marks, which are involved in the progression of early meiosis and spermiogenesis respectively (Hayashi et al., 2005; Bell et al., 2014), were present in a lesser proportion of spermatogonia, round and elongated spermatids and in a higher proportion of pachytene spermatocytes in cultures of fresh tissues compared to *in vivo* controls. It has been shown that a decrease in H3K4me3 or in H3K9ac could impair meiotic progression or induce morphological alterations and apoptosis in round spermatids respectively (Hayashi et al., 2005; Dai et al., 2015). This could explain, at least in part, the alteration of meiotic and postmeiotic progression and the presence of degenerating round spermatids in *in vitro* matured tissues as well as the low spermatogenic yield previously reported by us and others (Dumont et al., 2016; Rondanino et al., 2017; Yao et al., 2017). The acetylation of histones, which precedes histone-to-protamine replacement, was probably unaffected in the surviving spermatids since most of *in vitro* produced spermatozoa contain normally condensed chromatin (Oblette et al., 2017). Finally, while H4K8ac was found in less spermatogonia and leptotene/zygotene spermatocytes in our cultures of fresh tissues, the proportion of spermatids containing this mark was similar to *in vivo* controls. The freezing/thawing procedures used in this study also altered the distribution of the histone marks. A disturbed expression of histone modifying enzymes (PRDM9, JARID1B, SRC1, SIRT1, HDAC1 or others) or of their activity in organotypic cultures could explain these results.

Genome-wide single-cell methylome analysis and chromatin immunoprecipitation sequencing will be necessary to explore in more detail DNA methylation in *in vitro* produced spermatozoa, and especially the methylation status of imprinted genes, as well as the genomic distribution of modified histones.

In conclusion, we here report for the first time that germ cells go through DNA methylation and histone PTMs when *in vitro* matured. Importantly, in the context of fertility preservation, the present study was also performed on frozen/thawed samples. DNA methylation was found in cultures of frozen/thawed prepubertal testicular tissues and in spermatozoa generated in these tissues. Histone methylation and acetylation also occurred in germ cells in cultures of cryopreserved tissues. Before applying *in vitro* maturation to frozen/thawed prepubertal testicular tissues of pediatric cancer survivors, further studies will be necessary to investigate whether imprinted genes are properly methylated in *in vitro* produced spermatozoa, whether histone marks localize to the correct regions of the genome, and whether first and second-generation offspring are healthy, long-living and do not present behavioral disorders.

Vitae

Antoine Oblette is a PhD student in the Gametogenesis and Gamete Quality team within the Institute for Research and Innovation in Biomedicine and University Hospital of Rouen in France. His area of research covers fertility preservation and restoration in young boys with cancer.

List of abbreviations

CSF: controlled slow freezing; DNMT: DNA methyltransferase; d*pp*: days *postpartum*; FSH: follicle stimulating hormone; H3K4me3: trimethylated histone H3 on lysine 4; H3K9ac: acetylated histone H3 on lysine 9; H4K8ac: acetylated histone H4 on lysine 8; KSR: KnockOut serum replacement; 5mC: 5-methylcytosine; PTMs: post-translational modifications; Rol: retinol; SSC: spermatogonial stem cells; SSV: solid surface vitrification

Acknowledgements. The authors are grateful to Véronique Duchesne, Amandine Bironneau and Shirley Troche for excellent technical assistance.

Competing interests. The authors declare that they have no competing interests.

Authors' contributions. AO performed experiments, analyzed data and wrote the manuscript; JR performed experiments, analyzed data and revised the manuscript; LD, MD, JS and AR analyzed data and revised the manuscript; NR supervised the study and revised the manuscript; CR designed and supervised the study and wrote the manuscript. All the authors approved the final version of the manuscript.

Funding. This work was supported by Rouen University Hospital, Ligue contre le Cancer [to NR and AO], Agence de la Biomédecine [to NR], Association Laurette Fugain [to NR and CR], France Lymphome Espoir [to NR], and co-supported by European Union and Région Normandie [to AO]. Europe gets involved in Normandie with European Régional Development Fund (ERDF). The funding sources had no role in the design of the study, collection, analysis and interpretation of data, and in writing the manuscript.

687 **References**

688 Abu Elhija, M., Lunenfeld, E., Schlatt, S., Huleihel, M., 2012. Differentiation of murine male
689 germ cells to spermatozoa in a soft agar culture system. Asian J. Androl. 14, 285–
690 293. https://doi.org/10.1038/aja.2011.112
691 Arkoun, B., Dumont, L., Milazzo, J.-P., Rondanino, C., Bironneau, A., Wils, J., Rives, N.,
692 2016. Does soaking temperature during controlled slow freezing of pre-pubertal
693 mouse testes influence course of in vitro spermatogenesis? Cell Tissue Res. 364,
694 661–674. https://doi.org/10.1007/s00441-015-2341-2
695 Arkoun, B., Dumont, L., Milazzo, J.-P., Way, A., Bironneau, A., Wils, J., Macé, B., Rives, N.,
696 2015. Retinol improves in vitro differentiation of pre-pubertal mouse
697 spermatogonial stem cells into sperm during the first wave of spermatogenesis.
698 PLoS ONE 10, e0116660. https://doi.org/10.1371/journal.pone.0116660
699 Baert, Y., Goossens, E., van Saen, D., Ning, L., in't Veld, P., Tournaye, H., 2012. Orthotopic
700 grafting of cryopreserved prepubertal testicular tissue: in search of a simple yet
701 effective cryopreservation protocol. Fertil. Steril. 97, 1152-1157.e1–2.
702 https://doi.org/10.1016/j.fertnstert.2012.02.010
703 Bell, E.L., Nagamori, I., Williams, E.O., Del Rosario, A.M., Bryson, B.D., Watson, N., White,
704 F.M., Sassone-Corsi, P., Guarente, L., 2014. SirT1 is required in the male germ cell
705 for differentiation and fecundity in mice. Development 141, 3495–3504.
706 https://doi.org/10.1242/dev.110627
707 Boissonnas, C.C., Jouannet, P., Jammes, H., 2013. Epigenetic disorders and male
708 subfertility. Fertil. Steril. 99, 624–631.
709 https://doi.org/10.1016/j.fertnstert.2013.01.124
710 Champroux, A., Cocquet, J., Henry-Berger, J., Drevet, J.R., Kocer, A., 2018. A Decade of
711 Exploring the Mammalian Sperm Epigenome: Paternal Epigenetic and

712 Transgenerational Inheritance. Frontiers in Cell and Developmental Biology 6.
713 https://doi.org/10.3389/fcell.2018.00050
714 Cui, X., Jing, X., Wu, X., Yan, M., Li, Q., Shen, Y., Wang, Z., 2016. DNA methylation in
715 spermatogenesis and male infertility. Exp Ther Med 12, 1973–1979.
716 https://doi.org/10.3892/etm.2016.3569
717 Dai, L., Endo, D., Akiyama, N., Yamamoto-Fukuda, T., Koji, T., 2015. Aberrant levels of
718 histone H3 acetylation induce spermatid anomaly in mouse testis. Histochemistry
719 and Cell Biology 143, 209–224. https://doi.org/10.1007/s00418-014-1283-1
720 de Michele, F., Vermeulen, M., Wyns, C., 2017. Fertility restoration with spermatogonial
721 stem cells. Curr Opin Endocrinol Diabetes Obes 24, 424–431.
722 https://doi.org/10.1097/MED.0000000000000370
723 Dumont, L., Arkoun, B., Jumeau, F., Milazzo, J.-P., Bironneau, A., Liot, D., Wils, J.,
724 Rondanino, C., Rives, N., 2015. Assessment of the optimal vitrification protocol for
725 pre-pubertal mice testes leading to successful in vitro production of flagellated
726 spermatozoa. Andrology 3, 611–625. https://doi.org/10.1111/andr.12042
727 Dumont, L., Chalmel, F., Oblette, A., Berby, B., Rives, A., Duchesne, V., Rondanino, C.,
728 Rives, N., 2017. Evaluation of apoptotic- and autophagic-related protein
729 expressions before and after IVM of fresh, slow-frozen and vitrified pre-pubertal
730 mouse testicular tissue. Mol. Hum. Reprod. 23, 738–754.
731 https://doi.org/10.1093/molehr/gax054
732 Dumont, L., Oblette, A., Rondanino, C., Jumeau, F., Bironneau, A., Liot, D., Duchesne, V.,
733 Wils, J., Rives, N., 2016. Vitamin A prevents round spermatid nuclear damage and
734 promotes the production of motile sperm during in vitro maturation of vitrified
735 pre-pubertal mouse testicular tissue. Mol. Hum. Reprod. 22, 819–832.
736 https://doi.org/10.1093/molehr/gaw063

737 Gies, I., De Schepper, J., Tournaye, H., 2015. Progress and prospects for fertility
738 preservation in prepubertal boys with cancer. Curr Opin Endocrinol Diabetes
739 Obes 22, 203–208. https://doi.org/10.1097/MED.0000000000000162
740 Godmann, M., Auger, V., Ferraroni-Aguiar, V., Sauro, A.D., Sette, C., Behr, R., Kimmins, S.,
741 2007. Dynamic Regulation of Histone H3 Methylation at Lysine 4 in Mammalian
742 Spermatogenesis1. Biology of Reproduction 77, 754–764.
743 https://doi.org/10.1095/biolreprod.107.062265
744 Goossens, E., Bilgec, T., Van Saen, D., Tournaye, H., 2011. Mouse germ cells go through
745 typical epigenetic modifications after intratesticular tissue grafting. Hum. Reprod.
746 26, 3388–3400. https://doi.org/10.1093/humrep/der334
747 Goossens, E., De Rycke, M., Haentjens, P., Tournaye, H., 2009. DNA methylation patterns
748 of spermatozoa and two generations of offspring obtained after murine
749 spermatogonial stem cell transplantation. Hum. Reprod. 24, 2255–2263.
750 https://doi.org/10.1093/humrep/dep213
751 Goossens, E., Van Saen, D., Tournaye, H., 2013. Spermatogonial stem cell preservation
752 and transplantation: from research to clinic. Hum. Reprod. 28, 897–907.
753 https://doi.org/10.1093/humrep/det039
754 Gunes, S., Arslan, M.A., Hekim, G.N.T., Asci, R., 2016. The role of epigenetics in idiopathic
755 male infertility. J. Assist. Reprod. Genet. 33, 553–569.
756 https://doi.org/10.1007/s10815-016-0682-8
757 Hammoud, S.S., Nix, D.A., Hammoud, A.O., Gibson, M., Cairns, B.R., Carrell, D.T., 2011.
758 Genome-wide analysis identifies changes in histone retention and epigenetic
759 modifications at developmental and imprinted gene loci in the sperm of infertile
760 men. Human Reproduction 26, 2558–2569.
761 https://doi.org/10.1093/humrep/der192

762 Hayashi, K., Yoshida, K., Matsui, Y., 2005. A histone H3 methyltransferase controls
763 epigenetic events required for meiotic prophase. Nature 438, 374–378.
764 https://doi.org/10.1038/nature04112
765 Hazzouri, M., Pivot-Pajot, C., Faure, A.K., Usson, Y., Pelletier, R., Sèle, B., Khochbin, S.,
766 Rousseaux, S., 2000. Regulated hyperacetylation of core histones during mouse
767 spermatogenesis: involvement of histone deacetylases. Eur. J. Cell Biol. 79, 950–
768 960. https://doi.org/10.1078/0171-9335-00123
769 Ibtisham, F., Wu, J., Xiao, M., An, L., Banker, Z., Nawab, A., Zhao, Y., Li, G., 2017. Progress
770 and future prospect of in vitro spermatogenesis. Oncotarget 8, 66709–66727.
771 https://doi.org/10.18632/oncotarget.19640
772 Jahnukainen, K., Mitchell, R.T., Stukenborg, J.-B., 2015. Testicular function and fertility
773 preservation after treatment for haematological cancer. Curr Opin Endocrinol
774 Diabetes Obes 22, 217–223. https://doi.org/10.1097/MED.0000000000000156
775 Jenkins, T.G., Aston, K.I., James, E.R., Carrell, D.T., 2017. Sperm epigenetics in the study of
776 male fertility, offspring health, and potential clinical applications. Syst Biol
777 Reprod Med 63, 69–76. https://doi.org/10.1080/19396368.2016.1274791
778 Jenkins, T.G., Carrell, D.T., 2012. The sperm epigenome and potential implications for the
779 developing embryo. Reproduction 143, 727–734. https://doi.org/10.1530/REP-
780 11-0450
781 Kitamura, A., Miyauchi, N., Hamada, H., Hiura, H., Chiba, H., Okae, H., Sato, A., John, R.M.,
782 Arima, T., 2015. Epigenetic alterations in sperm associated with male infertility.
783 Congenit Anom (Kyoto) 55, 133–144. https://doi.org/10.1111/cga.12113
784 Kubo, N., Toh, H., Shirane, K., Shirakawa, T., Kobayashi, H., Sato, T., Sone, H., Sato, Y.,
785 Tomizawa, S., Tsurusaki, Y., Shibata, H., Saitsu, H., Suzuki, Y., Matsumoto, N.,
786 Suyama, M., Kono, T., Ohbo, K., Sasaki, H., 2015. DNA methylation and gene

787 expression dynamics during spermatogonial stem cell differentiation in the early
788 postnatal mouse testis. BMC Genomics 16, 624. https://doi.org/10.1186/s12864-
789 015-1833-5
790 La Salle, S., Mertineit, C., Taketo, T., Moens, P.B., Bestor, T.H., Trasler, J.M., 2004.
791 Windows for sex-specific methylation marked by DNA methyltransferase
792 expression profiles in mouse germ cells. Dev. Biol. 268, 403–415.
793 https://doi.org/10.1016/j.ydbio.2003.12.031
794 La Salle, S., Trasler, J.M., 2006. Dynamic expression of DNMT3a and DNMT3b isoforms
795 during male germ cell development in the mouse. Dev. Biol. 296, 71–82.
796 https://doi.org/10.1016/j.ydbio.2006.04.436
797 Langenstroth-Röwer, D., Gromoll, J., Wistuba, J., Tröndle, I., Laurentino, S., Schlatt, S.,
798 Neuhaus, N., 2017. De novo methylation in male germ cells of the common
799 marmoset monkey occurs during postnatal development and is maintained in
800 vitro. Epigenetics 12, 527–539.
801 https://doi.org/10.1080/15592294.2016.1248007
802 Liu, C., Song, Z., Wang, L., Yu, H., Liu, W., Shang, Y., Xu, Z., Zhao, H., Gao, Fengyi, Wen, J.,
803 Zhao, L., Gui, Y., Jiao, J., Gao, Fei, Li, W., 2017. Sirt1 regulates acrosome biogenesis
804 by modulating autophagic flux during spermiogenesis in mice. Development 144,
805 441–451. https://doi.org/10.1242/dev.147074
806 Livera, G., Rouiller-Fabre, V., Pairault, C., Levacher, C., Habert, R., 2002. Regulation and
807 perturbation of testicular functions by vitamin A. Reproduction 124, 173–180.
808 Luense, L.J., Wang, X., Schon, S.B., Weller, A.H., Lin Shiao, E., Bryant, J.M., Bartolomei, M.S.,
809 Coutifaris, C., Garcia, B.A., Berger, S.L., 2016. Comprehensive analysis of histone
810 post-translational modifications in mouse and human male germ cells.
811 Epigenetics & Chromatin 9. https://doi.org/10.1186/s13072-016-0072-6

McSwiggin, H.M., O'Doherty, A.M., 2018. Epigenetic reprogramming during spermatogenesis and male factor infertility. Reproduction 156, R9–R21. https://doi.org/10.1530/REP-18-0009

Mertineit, C., Yoder, J.A., Taketo, T., Laird, D.W., Trasler, J.M., Bestor, T.H., 1998. Sex-specific exons control DNA methyltransferase in mammalian germ cells. Development 125, 889–897.

Milazzo, J.P., Travers, A., Bironneau, A., Safsaf, A., Gruel, E., Arnoult, C., Mace, B., Boyer, O., Rives, N., 2010. Rapid Screening of Cryopreservation Protocols for Murine Prepubertal Testicular Tissue by Histology and PCNA Immunostaining. Journal of Andrology 31, 617–630. https://doi.org/10.2164/jandrol.109.009324

Milazzo, J.P., Vaudreuil, L., Cauliez, B., Gruel, E., Massé, L., Mousset-Siméon, N., Macé, B., Rives, N., 2008. Comparison of conditions for cryopreservation of testicular tissue from immature mice. Hum. Reprod. 23, 17–28. https://doi.org/10.1093/humrep/dem355

Nurmio, M., Keros, V., Lähteenmäki, P., Salmi, T., Kallajoki, M., Jahnukainen, K., 2009. Effect of Childhood Acute Lymphoblastic Leukemia Therapy on Spermatogonia Populations and Future Fertility. J Clin Endocrinol Metab 94, 2119–2122. https://doi.org/10.1210/jc.2009-0060

Oblette, A., Rives, N., Dumont, L., Rives, A., Verhaeghe, F., Jumeau, F., Rondanino, C., 2017. Assessment of sperm nuclear quality after in vitro maturation of fresh or frozen/thawed mouse pre-pubertal testes. Mol. Hum. Reprod. 23, 674–684. https://doi.org/10.1093/molehr/gax048

Onofre, J., Baert, Y., Faes, K., Goossens, E., 2016. Cryopreservation of testicular tissue or testicular cell suspensions: a pivotal step in fertility preservation. Hum. Reprod. Update 22, 744–761. https://doi.org/10.1093/humupd/dmw029

837 Picton, H.M., Wyns, C., Anderson, R.A., Goossens, E., Jahnukainen, K., Kliesch, S., Mitchell,
838 R.T., Pennings, G., Rives, N., Tournaye, H., van Pelt, A.M.M., Eichenlaub-Ritter, U.,
839 Schlatt, S., ESHRE Task Force On Fertility Preservation In Severe Diseases, 2015.
840 A European perspective on testicular tissue cryopreservation for fertility
841 preservation in prepubertal and adolescent boys. Hum. Reprod. 30, 2463–2475.
842 https://doi.org/10.1093/humrep/dev190
843 Poels, J., Van Langendonckt, A., Many, M.-C., Wese, F.-X., Wyns, C., 2013. Vitrification
844 preserves proliferation capacity in human spermatogonia. Hum. Reprod. 28, 578–
845 589. https://doi.org/10.1093/humrep/des455
846 Rondanino, C., Maouche, A., Dumont, L., Oblette, A., Rives, N., 2017. Establishment,
847 maintenance and functional integrity of the blood-testis barrier in organotypic
848 cultures of fresh and frozen/thawed prepubertal mouse testes. Mol. Hum.
849 Reprod. 23, 304–320. https://doi.org/10.1093/molehr/gax017
850 Rwigemera, A., Joao, F., Delbes, G., 2017. Fetal testis organ culture reproduces the
851 dynamics of epigenetic reprogramming in rat gonocytes. Epigenetics Chromatin
852 10, 19. https://doi.org/10.1186/s13072-017-0127-3
853 Sanjo, H., Komeya, M., Sato, T., Abe, T., Katagiri, K., Yamanaka, H., Ino, Y., Arakawa, N.,
854 Hirano, H., Yao, T., Asayama, Y., Matsuhisa, A., Yao, M., Ogawa, T., 2018. In vitro
855 mouse spermatogenesis with an organ culture method in chemically defined
856 medium. PLoS ONE 13, e0192884.
857 https://doi.org/10.1371/journal.pone.0192884
858 Santi, D., De Vincentis, S., Magnani, E., Spaggiari, G., 2017. Impairment of sperm DNA
859 methylation in male infertility: a meta-analytic study. Andrology 5, 695–703.
860 https://doi.org/10.1111/andr.12379

Sato, T., Katagiri, K., Gohbara, A., Inoue, K., Ogonuki, N., Ogura, A., Kubota, Y., Ogawa, T., 2011. In vitro production of functional sperm in cultured neonatal mouse testes. Nature 471, 504–507. https://doi.org/10.1038/nature09850

Sonnack, V., Failing, K., Bergmann, M., Steger, K., 2002. Expression of hyperacetylated histone H4 during normal and impaired human spermatogenesis. Andrologia 34, 384–390.

Steilmann, C., Paradowska, A., Bartkuhn, M., Vieweg, M., Schuppe, H.-C., Bergmann, M., Kliesch, S., Weidner, W., Steger, K., 2011. Presence of histone H3 acetylated at lysine 9 in male germ cells and its distribution pattern in the genome of human spermatozoa. Reproduction, Fertility and Development 23, 997. https://doi.org/10.1071/RD10197

Stewart, K.R., Veselovska, L., Kelsey, G., 2016. Establishment and functions of DNA methylation in the germline. Epigenomics 8, 1399–1413. https://doi.org/10.2217/epi-2016-0056

Stuppia, L., Franzago, M., Ballerini, P., Gatta, V., Antonucci, I., 2015. Epigenetics and male reproduction: the consequences of paternal lifestyle on fertility, embryo development, and children lifetime health. Clin Epigenetics 7, 120. https://doi.org/10.1186/s13148-015-0155-4

Uysal, F., Akkoyunlu, G., Ozturk, S., 2016. DNA methyltransferases exhibit dynamic expression during spermatogenesis. Reprod. Biomed. Online 33, 690–702. https://doi.org/10.1016/j.rbmo.2016.08.022

Vieweg, M., Dvorakova-Hortova, K., Dudkova, B., Waliszewski, P., Otte, M., Oels, B., Hajimohammad, A., Turley, H., Schorsch, M., Schuppe, H.-C., Weidner, W., Steger, K., Paradowska-Dogan, A., 2015. Methylation analysis of histone H4K12ac-

885 associated promoters in sperm of healthy donors and subfertile patients. Clinical
886 Epigenetics 7, 31. https://doi.org/10.1186/s13148-015-0058-4
887 Watanabe, D., Suetake, I., Tajima, S., Hanaoka, K., 2004. Expression of Dnmt3b in mouse
888 hematopoietic progenitor cells and spermatogonia at specific stages. Gene Expr.
889 Patterns 5, 43–49. https://doi.org/10.1016/j.modgep.2004.06.008
890 Wyns, C., Collienne, C., Shenfield, F., Robert, A., Laurent, P., Roegiers, L., Brichard, B.,
891 2015. Fertility preservation in the male pediatric population: factors influencing
892 the decision of parents and children. Hum. Reprod. 30, 2022–2030.
893 https://doi.org/10.1093/humrep/dev161
894 Wyns, C., Curaba, M., Vanabelle, B., Van Langendonckt, A., Donnez, J., 2010. Options for
895 fertility preservation in prepubertal boys. Hum. Reprod. Update 16, 312–328.
896 https://doi.org/10.1093/humupd/dmp054
897 Yao, C., Liu, Y., Sun, M., Niu, M., Yuan, Q., Hai, Y., Guo, Y., Chen, Z., Hou, J., Liu, Y., He, Z.,
898 2015. MicroRNAs and DNA methylation as epigenetic regulators of mitosis,
899 meiosis and spermiogenesis. Reproduction 150, R25–R34.
900 https://doi.org/10.1530/REP-14-0643
901 Yao, J., Zuo, H., Gao, J., Wang, M., Wang, D., Li, X., 2017. The effects of IGF-1 on mouse
902 spermatogenesis using an organ culture method. Biochem. Biophys. Res.
903 Commun. https://doi.org/10.1016/j.bbrc.2017.05.125
904 Yokonishi, T., Ogawa, T., 2016. Cryopreservation of testis tissues and in vitro
905 spermatogenesis. Reprod. Med. Biol. 15, 21–28.
906 https://doi.org/10.1007/s12522-015-0218-4
907 Yokonishi, T., Sato, T., Komeya, M., Katagiri, K., Kubota, Y., Nakabayashi, K., Hata, K.,
908 Inoue, K., Ogonuki, N., Ogura, A., Ogawa, T., 2014. Offspring production with

sperm grown in vitro from cryopreserved testis tissues. Nat Commun 5, 4320. https://doi.org/10.1038/ncomms5320

Zhang, L., Wang, J., Pan, Y., Jin, J., Sang, J., Huang, P., Shao, G., 2014. Expression of histone H3 lysine 4 methylation and its demethylases in the developing mouse testis. Cell and Tissue Research 358, 875–883. https://doi.org/10.1007/s00441-014-1991-9

Figure legends

Figure 1. Expression of epigenetic modification enzymes, DNA methylation and histone post-translational modifications in fresh and frozen/thawed prepubertal mouse testes.

(**A**) Relative mRNA levels of the *Dnmt1* and *Dnmt3a* genes normalized to the housekeeping gene *Gapdh* in fresh, CSF and SSV 6-7 d*pp* testes (n=3). Histograms are expressed as mean ± SD. **P* < 0.05.

(**B**) Relative mRNA levels of the *Prdm9*, *Jarid1b*, *Src1*, *Sirt1* and *Hdac1* genes normalized to the housekeeping gene *Gapdh* in fresh, CSF and SSV 6-7 d*pp* testes (n=3). Histograms are expressed as mean ± SD. **P* < 0.05.

(**C**) Localization of DNMT1, DNMT3a and the 5mC, H3K4me3, H3K9ac and H4K8ac epigenetic marks in fresh, CSF and SSV 6-7 d*pp* testes (n=4). Shown are representative microscopy images of DNMT1, DNMT3a, 5mC, H3K4me3, H3K9ac and H4K8ac labelling. Antibody binding was visualized using 3,3'-diaminobenzidine (brown staining) and tissue sections were counterstained with hematoxylin. Enlarged views of labelled and unlabeled spermatogonia are shown in the upper right corner and in the lower right corner, respectively. Bar: 50 μm.

(**D**) Proportion of DNMT1, DNMT3a and 5mC-positive spermatogonia in 30 cross-sectioned seminiferous tubules of fresh, CSF and SSV 6-7 d*pp* testes (n=4). Histograms are expressed as mean ± SD. *$P < 0.05$.

(**E**) Proportion of H3K4me3, H3K9ac and H4K8ac-positive spermatogonia in 30 cross-sectioned seminiferous tubules of fresh, CSF and SSV 6-7 d*pp* testes (n=4). Histograms are expressed as mean ± SD. *$P < 0.05$.

CSF: controlled slow freezing; *Dnmt*/DNMT: DNA methyltransferase; d*pp*: days *postpartum*; *Gapdh*: Glyceraldehyde-3-phosphate dehydrogenase; H3K4me3: trimethylated histone H3 on lysine 4; H3K9ac: acetylated histone H3 on lysine 9; H4K8ac: acetylated histone H4 on lysine 8; *Hdac1*: Histone deacetylase 1; *Jarid1b*: Jumonji AT-rich interactive domain 1b; 5mC: 5-methylcytosine; *Prdm9*: PR domain-containing 9; *Sirt1*: Sirtuin 1; *Src1*: Steroid receptor coactivator 1; SSV: solid surface vitrification

Figure 2. Expression of genes encoding epigenetic modification enzymes in cultured testicular tissues and *in vivo* controls.

Relative mRNA levels of the (**A**) *Dnmt* genes (*Dnmt1*, *Dnmt3a*) and (**B**) genes encoding histone modifying enzymes (*Prdm9*, *Jarid1b*, *Src1*, *Sirt1*, *Hdac1*) normalized to the housekeeping gene *Gapdh* in 30-day cultures of fresh, CSF or SSV testicular fragments with retinol (n = 3) and in testes of mice aged 36–37 d*pp* (n = 3). Histograms are expressed as mean ± SD. *$P < 0.05$, **$P < 0.01$.

CSF: controlled slow freezing; D30: day 30; *Dnmt*: DNA methyltransferase; d*pp*: days *postpartum*; *Gapdh*: Glyceraldehyde-3-phosphate dehydrogenase; *Hdac1*: Histone deacetylase 1; *Jarid1b*: Jumonji AT-rich interactive domain 1b; *Prdm9*: PR domain-containing 9; Rol: retinol; *Sirt1*: Sirtuin 1; *Src1*: Steroid receptor coactivator 1; SSV: solid surface vitrification

Figure 3. Immunolocalization of DNMT1, DNMT3a and 5mC in cultures of fresh prepubertal testes and *in vivo*.

(**A**) Localization of DNMT1, DNMT3a and the 5mC epigenetic mark in fresh testicular fragments cultured for 30 days with retinol (n=4) and in 36-37 d*pp* testes (*in vivo* controls, n=4). Shown are representative microscopy images of DNMT1, DNMT3a and 5mC labelling. Antibody binding was visualized using 3,3'-diaminobenzidine (brown staining) and tissue sections were counterstained with hematoxylin. Enlarged views of spermatogonia and leptotene/zygotene spermatocytes are shown in the upper right corner and in the lower right corner, respectively. Bar: 50 μm.

(**B**) Proportion of DNMT1, DNMT3a and 5mC-positive spermatogonia and leptotene/zygotene spermatocytes in 30-day cultures of fresh testicular fragments with retinol (n=4) and in control 36-37 d*pp* testes (n=4). The localization of DNMT1, DNMT3a and 5mC was analyzed in 30 cross-sectioned seminiferous tubules from three sections. Histograms are expressed as mean ± SD. *$P < 0.05$.

D30: day 30; DNMT: DNA methyltransferase; d*pp*: days *postpartum*; 5mC: 5-methylcytosine; L/Z: leptotene/zygotene spermatocyte; P: pachytene spermatocyte; Rol: retinol; Sg: spermatogonia

Figure 4. Immunolocalization of H3K4me3, H3K9ac and H4K8ac in cultures of fresh prepubertal testes and *in vivo*.

(**A**) Localization of the epigenetic marks H3K4me3, H3K9ac and H4K8ac in fresh testicular fragments cultured for 30 days with retinol (n=4) and in 36-37 d*pp* testes (*in vivo* controls, n=4). Shown are representative microscopy images of H3K4me3, H3K9ac and H4K8ac labelling. Antibody binding was visualized using 3,3'-diaminobenzidine (brown staining) and

983 tissue sections were counterstained with hematoxylin. Enlarged views of spermatogonia,
984 leptotene/zygotene and pachytene spermatocytes (upper right corner) and of round and
985 elongated spermatids (lower right corner) are shown. Bar: 50 µm.
986 (**B-D**) Proportion of (**B**) H3K4me3, (**C**) H3K9ac and (**D**) H4K8ac-positive spermatogonia,
987 leptotene/zygotene and pachytene spermatocytes, round and elongated spermatids in 30-day
988 cultures of fresh testicular fragments with retinol (n=4) and in control 36-37 d*pp* testes (n=4).
989 The localization of H3K4me3, H3K9ac and H4K8ac was analyzed in 30 cross-sectioned
990 seminiferous tubules from three sections. Histograms are expressed as mean ± SD. *$P < 0.05$,
991 **$P < 0.01$.
992 D30: day 30; d*pp*: days *postpartum*; ES: elongated spermatid; H3K4me3: trimethylated
993 histone H3 on lysine 4; H3K9ac: acetylated histone H3 on lysine 9; H4K8ac: acetylated
994 histone H4 on lysine 8; L/Z: leptotene/zygotene spermatocyte; P: pachytene spermatocyte;
995 Rol: retinol; RS: round spermatid; Sg: spermatogonia
996
997 **Figure 5.** Immunolocalization of DNMT1, DNMT3a and 5mC in 30-day cultures of
998 frozen/thawed prepubertal testes.
999 (**A**) Localization of DNMT1, DNMT3a and 5mC in CSF or SSV testicular fragments cultured
1000 for 30 days with retinol (n=4). Shown are representative microscopy images of DNMT1,
1001 DNMT3a and 5mC labelling. Antibody binding was visualized using 3,3'-diaminobenzidine
1002 (brown staining) and tissue sections were counterstained with hematoxylin. Enlarged views of
1003 spermatogonia and leptotene/zygotene spermatocytes are shown in the upper right corner and
1004 in the lower right corner, respectively. Bar: 50 µm.
1005 (**B**) Proportion of DNMT1, DNMT3a and 5mC-positive spermatogonia and
1006 leptotene/zygotene spermatocytes in CSF or SSV testicular fragments cultured for 30 days
1007 with retinol (n=4). The localization of DNMT1, DNMT3a and 5mC was analyzed in 30 cross-

sectioned seminiferous tubules from three sections. Histograms are expressed as mean ± SD. *$P < 0.05$.

CSF: controlled slow freezing; D30: day 30; DNMT: DNA methyltransferase; d*pp*: days *postpartum*; 5mC: 5-methylcytosine; L/Z: leptotene/zygotene spermatocyte; P: pachytene spermatocyte; Rol: retinol; Sg: spermatogonia; SSV: solid surface vitrification

Figure 6. Immunolocalization of H3K4me3, H3K9ac and H4K8ac in cultures of frozen/thawed prepubertal testes.

(**A**) Localization of H3K4me3, H3K9ac and H4K8ac in CSF or SSV testicular fragments cultured for 30 days with retinol (n=4). Shown are representative microscopy images of H3K4me3, H3K9ac and H4K8ac labelling. Antibody binding was visualized using 3,3'-diaminobenzidine (brown staining) and tissue sections were counterstained with hematoxylin. Enlarged views of spermatogonia, leptotene/zygotene and pachytene spermatocytes (upper right corner) and of round and elongated spermatids (lower right corner) are shown. Bar: 50 µm.

(**B-D**) Proportion of (**B**) H3K4me3, (**C**) H3K9ac and (**D**) H4K8ac-positive spermatogonia, leptotene/zygotene and pachytene spermatocytes, round and elongated spermatids in CSF and SSV fragments cultured for 30 days with retinol (n=4). The localization of H3K4me3, H3K9ac and H4K8ac was analyzed in 30 cross-sectioned seminiferous tubules from three sections. Histograms are expressed as mean ± SD. *$P < 0.05$.

D30: day 30; d*pp*: days *postpartum*; ES: elongated spermatid; H3K4me3: trimethylated histone H3 on lysine 4; H3K9ac: acetylated histone H3 on lysine 9; H4K8ac: acetylated histone H4 on lysine 8; L/Z: leptotene/zygotene; P: pachytene spermatocyte; Rol: retinol; RS: round spermatid; Sg: spermatogonia

Figure 7. DNA methylation in *in vitro* produced spermatozoa and *in vivo* controls.

(**A**) 5mC patterns in spermatozoa extracted from fresh, CSF or SSV testes after 30 days of culture in the presence of retinol, and from 36-37 d*pp* testes (*in vivo* controls). A hundred spermatozoa (from a pool of 6 *in vitro* matured testes or from 6 *in vivo* testes) were examined. Shown are representative images of 5mC immunofluorescence staining (in green) in spermatozoa. Cell nuclei were stained with DAPI (in blue). Representative merged fluorescent images obtained when the primary antibody was omitted (negative controls) are also shown (right column). Magnification: ×900, bar: 10 µm.

(**B**) Box plot distributions of normalized 5mC fluorescence intensity in spermatozoa extracted from fresh, CSF or SSV testes after 30 days of culture in the presence of retinol, and from 36-37 d*pp* testes (*in vivo* controls). The boxes stretch from the 25th to the 75th percentile. The median is shown as a line across the boxes. The horizontal lines outside the boxes display minimum and maximum. The circles represent outliers. $^{**}P < 0.01$.

CSF: controlled slow freezing; D30: day 30; DAPI: 4',6-diamidino-2-phenylindole; d*pp*: day *postpartum*; 5mC: 5-methylcytosine; Rol: retinol; SSV: solid surface vitrification

Additional File 1. Schematic representation of the experimental design

Testes from 6-7 d*pp* prepubertal CD-1 mice were obtained and organotypic cultures were performed either directly (from fresh tissues) or after thawing of testes frozen by CSF or SSV. Testicular fragments were cultured at a gas-liquid interphase on agarose gels (under 5% CO_2 at 34°C), with retinol alone or a retinol/FSH alternation ("Rol" and "Rol/FSH" culture conditions, respectively) for 30 days. Testes from mice aged 36-37 d*pp* represent the corresponding *in vivo* controls. After selection of the best culture condition, *in vitro* matured testicular tissues and *in vivo* controls were analyzed by RT-qPCR and by immunohistochemistry. Moreover, a hundred spermatozoa extracted from a pool of 6 *in vitro*

cultured testes or from 6 *in vivo* testes were analyzed by immunofluorescence. In order to evaluate the impact of the freezing procedures on the testicular tissues before culture, fresh, CSF and SSV testes from mice aged 6-7 d*pp* were also analyzed by RT-qPCR and immunohistochemistry. A total of 134 testes from 73 mice were used in this study. RT-qPCR analyses were repeated 3 times (from 3 different testes) and immunohistochemical analyses were repeated 4 times (from 4 different testes). For the analysis of sperm DNA methylation, a pool of 6 testes (from 6 different mice) was used to extract spermatozoa.

(*) The same testicular samples were used for the evaluation of spermatogenic progression and for DNMT1, DNMT3a, 5mC immunostaining

α-MEM: minimum essential medium α; CSF: controlled slow freezing; d*pp*: days *postpartum*; *Dnmt*/DNMT: DNA methyltransferase; FSH: follicle stimulating hormone; H3K4me3: trimethylated histone H3 on lysine 4; H3K9ac: acetylated histone H3 on lysine 9; H4K8ac: acetylated histone H4 on lysine 8; *Hdac1*: Histone deacetylase 1; *Jarid1b*: Jumonji AT-rich interactive domain 1b; KSR: *knockout* replacement serum; 5mC: 5-methylcytosine; *Prdm9*: PR domain-containing 9; Rol: retinol; RT-qPCR: quantitative PCR after reverse transcription; *Sirt1*: Sirtuin 1; *Src1*: Steroid receptor coactivator 1; SSV: solid surface vitrification

Figure 1

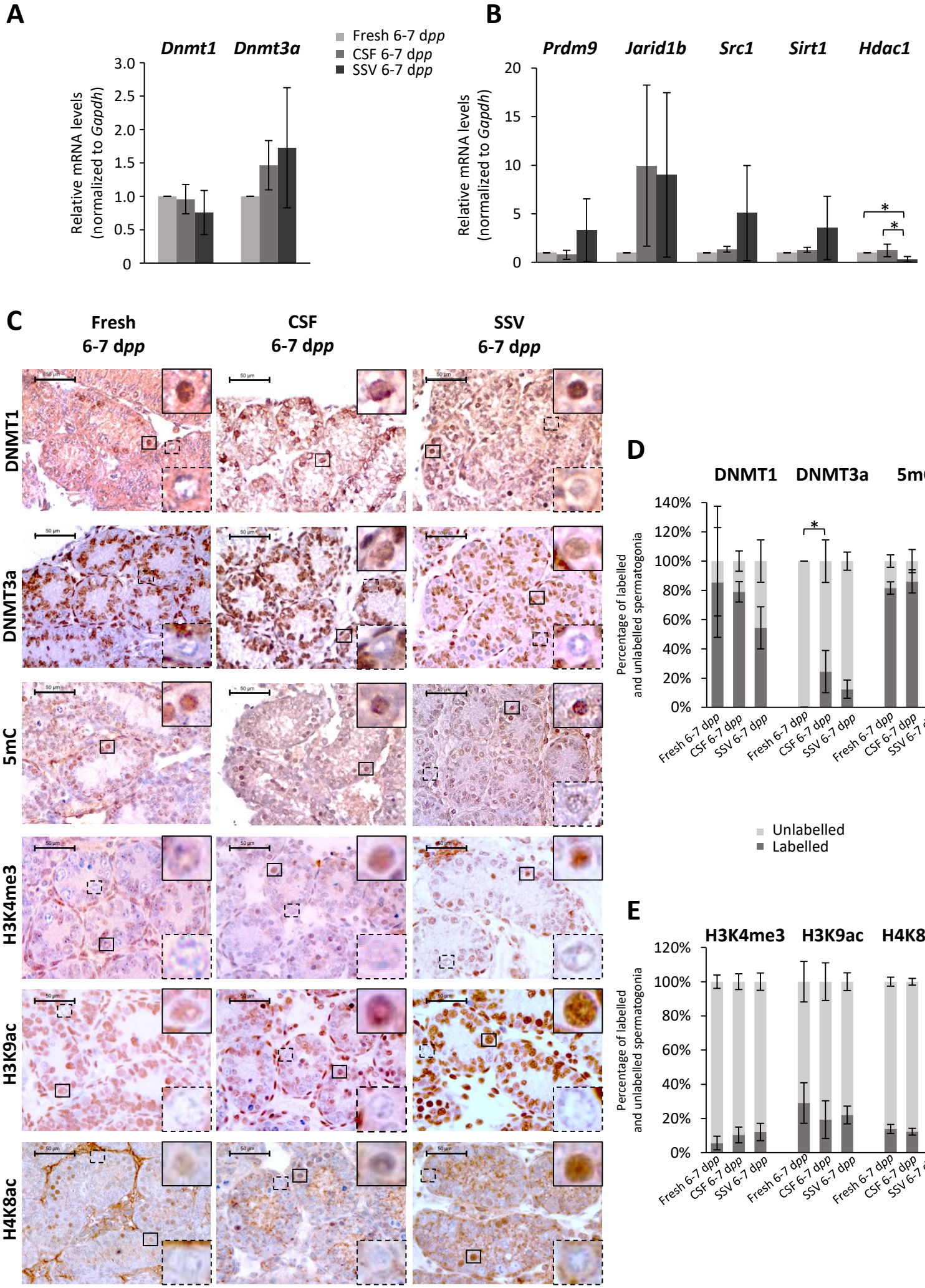
A
Dnmt1
Dnmt3a
Fresh 6-7 dpp
CSF 6-7 dpp
SSV 6-7 dpp
Relative mRNA levels (normalized to Gapdh)
3.0
2.5
2.0
1.5
1.0
0.5
0
B
Prdm9
Jarid1b
Src1
Sirt1
Hdac1
Relative mRNA levels (normalized to Gapdh)
20
15
10
5
0
*
*
C
Fresh 6-7 dpp
CSF 6-7 dpp
SSV 6-7 dpp
DNMT1
DNMT3a
5mC
H3K4me3
H3K9ac
H4K8ac
50 µm
D
DNMT1
DNMT3a
5mC
Percentage of labelled and unlabelled spermatogonia
140%
120%
100%
80%
60%
40%
20%
0%
*
Fresh 6-7 dpp
CSF 6-7 dpp
SSV 6-7 dpp
Unlabelled
Labelled
E
H3K4me3
H3K9ac
H4K8ac
Percentage of labelled and unlabelled spermatogonia
120%
100%
80%
60%
40%
20%
0%
Fresh 6-7 dpp
CSF 6-7 dpp
SSV 6-7 dpp

Figure 2

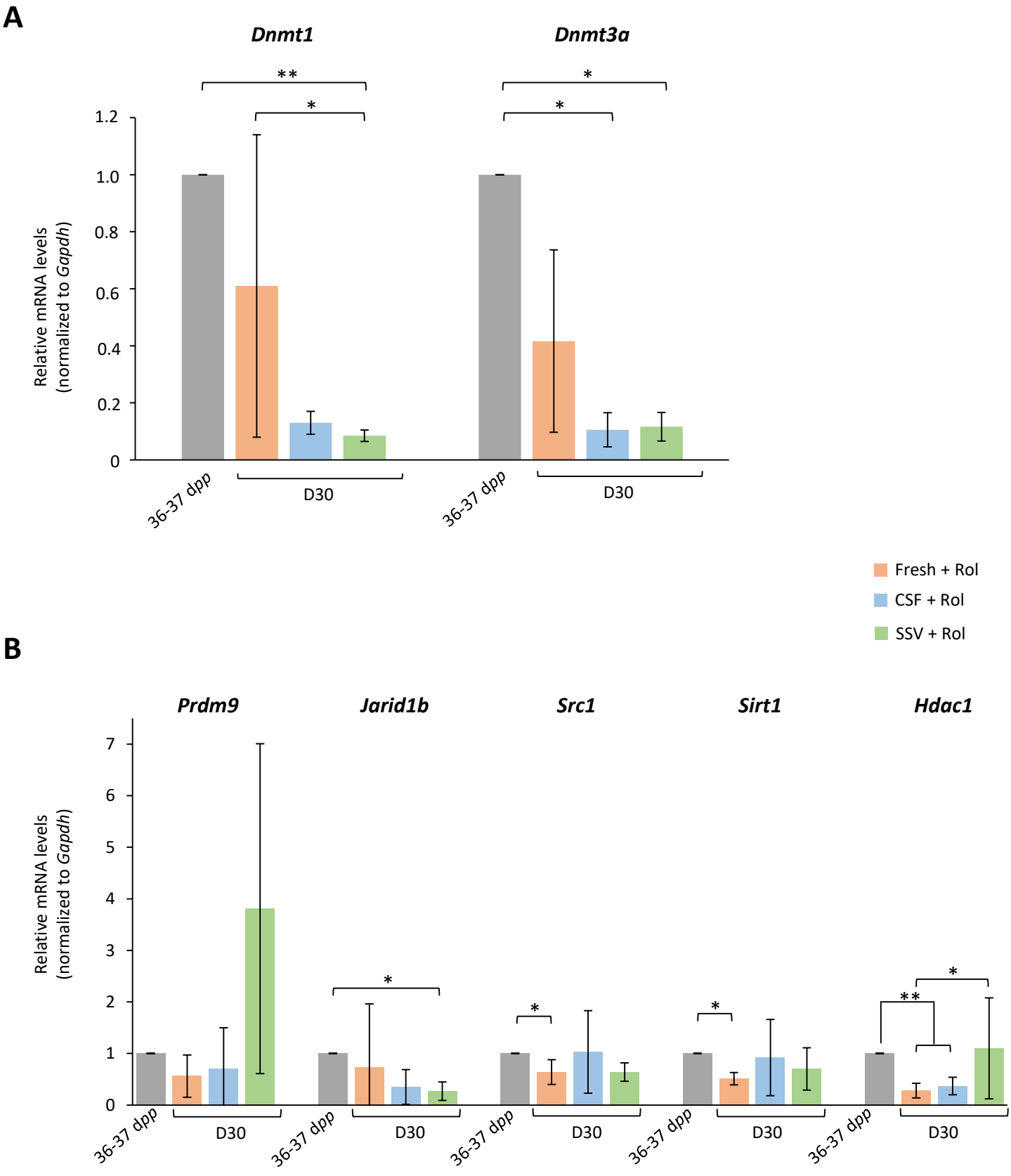
A
Dnmt1
Dnmt3a
Relative mRNA levels
(normalized to Gapdh)
1.2
1.0
0.8
0.6
0.4
0.2
0
**
*
*
*
36-37 dpp
D30
36-37 dpp
D30
Fresh + Rol
CSF + Rol
SSV + Rol
B
Prdm9
Jarid1b
Src1
Sirt1
Hdac1
Relative mRNA levels
(normalized to Gapdh)
7
6
5
4
3
2
1
0
*
*
*
**
*
36-37 dpp
D30
36-37 dpp
D30
36-37 dpp
D30
36-37 dpp
D30
36-37 dpp
D30

Figure 3

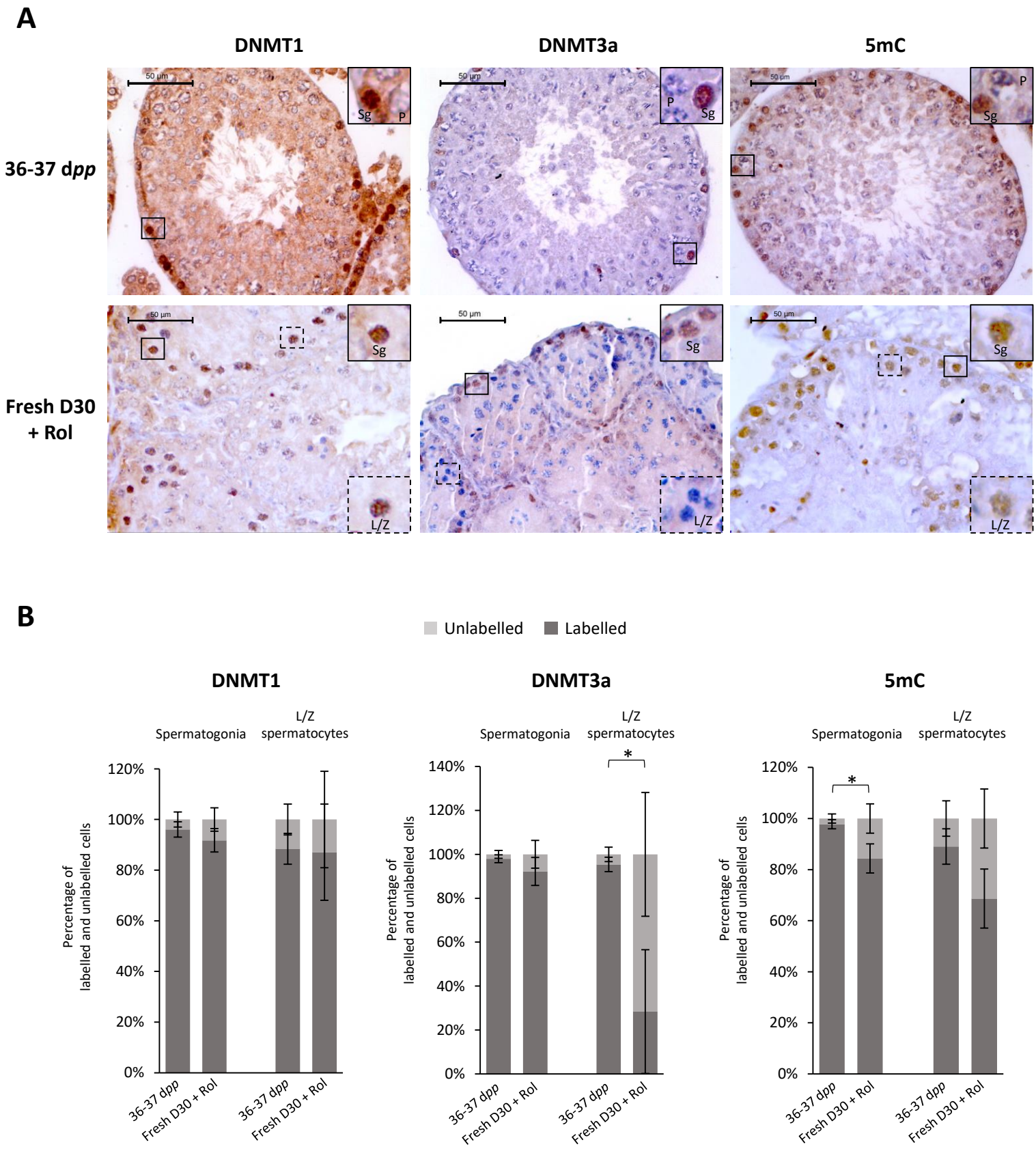
A
DNMT1
DNMT3a
5mC
36-37 dpp
Fresh D30 + Rol
50 µm
Sg
P
L/Z
B
Unlabelled
Labelled
DNMT1
DNMT3a
5mC
Spermatogonia
L/Z spermatocytes
Percentage of labelled and unlabelled cells
120%
100%
80%
60%
40%
20%
0%
140%
*
36-37 dpp
Fresh D30 + Rol

Figure 4

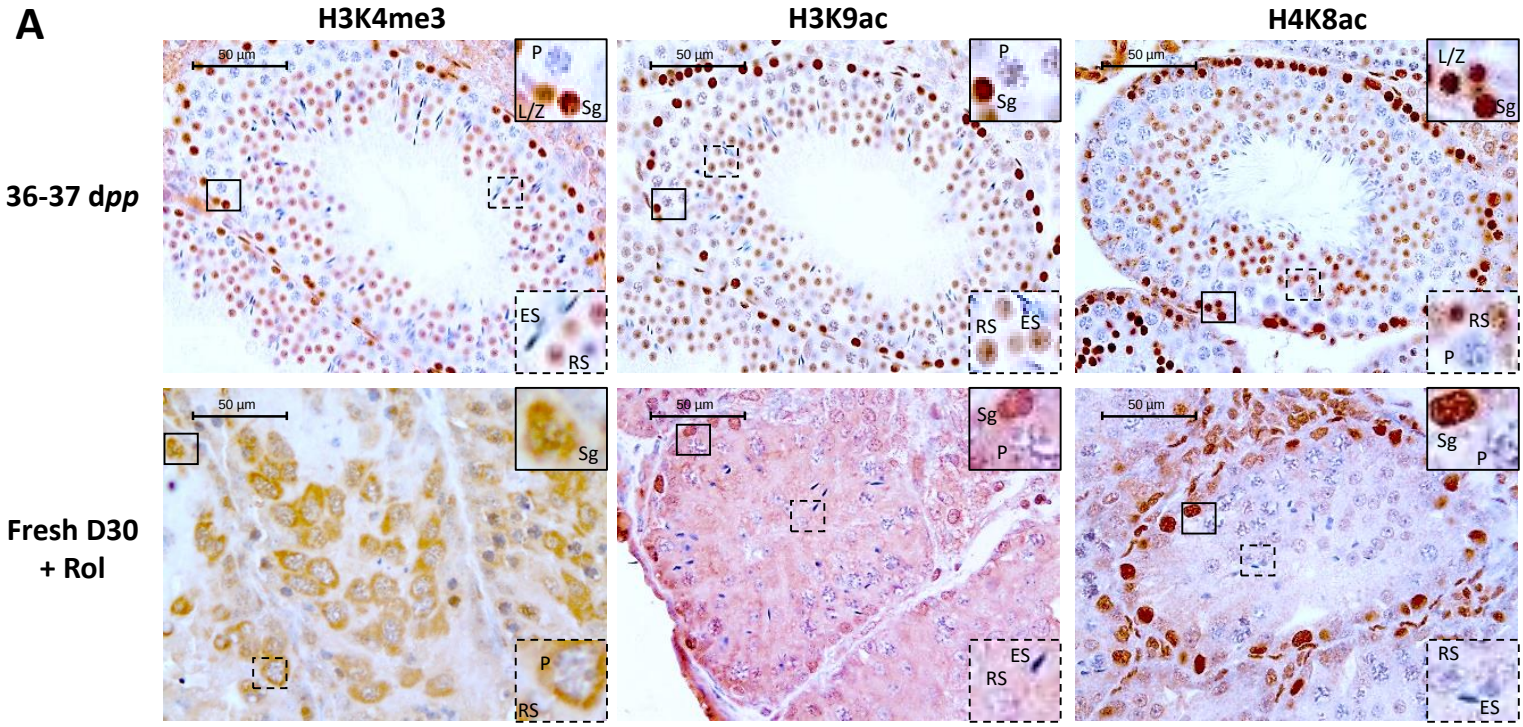
A
H3K4me3
H3K9ac
H4K8ac
36-37 dpp
Fresh D30 + Rol
50 µm
P
L/Z
Sg
ES
RS

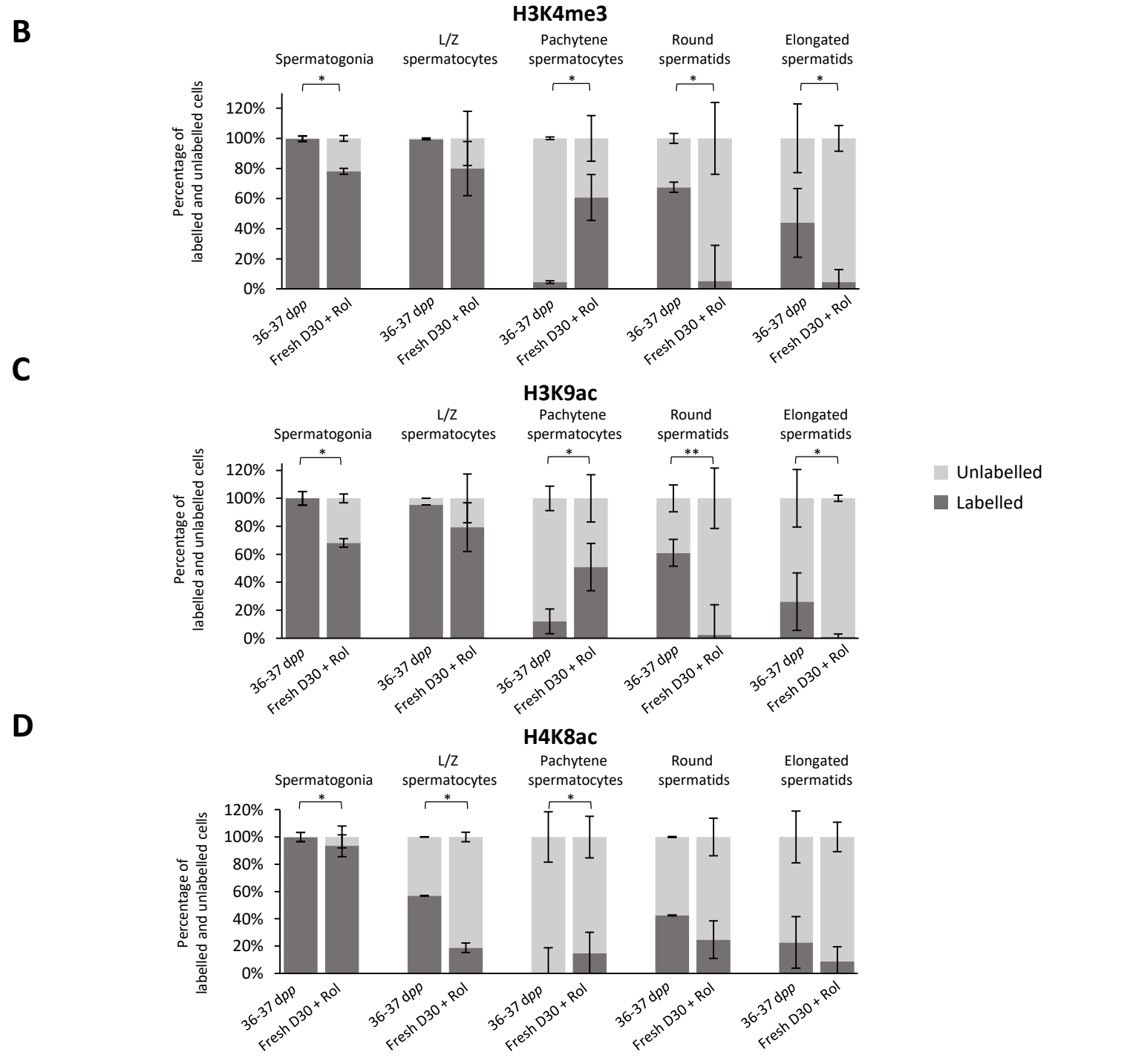
B
H3K4me3
C
H3K9ac
D
H4K8ac
Spermatogonia
L/Z spermatocytes
Pachytene spermatocytes
Round spermatids
Elongated spermatids
Percentage of labelled and unlabelled cells
120%
100%
80%
60%
40%
20%
0%
36-37 dpp
Fresh D30 + Rol
Unlabelled
Labelled

Figure 5

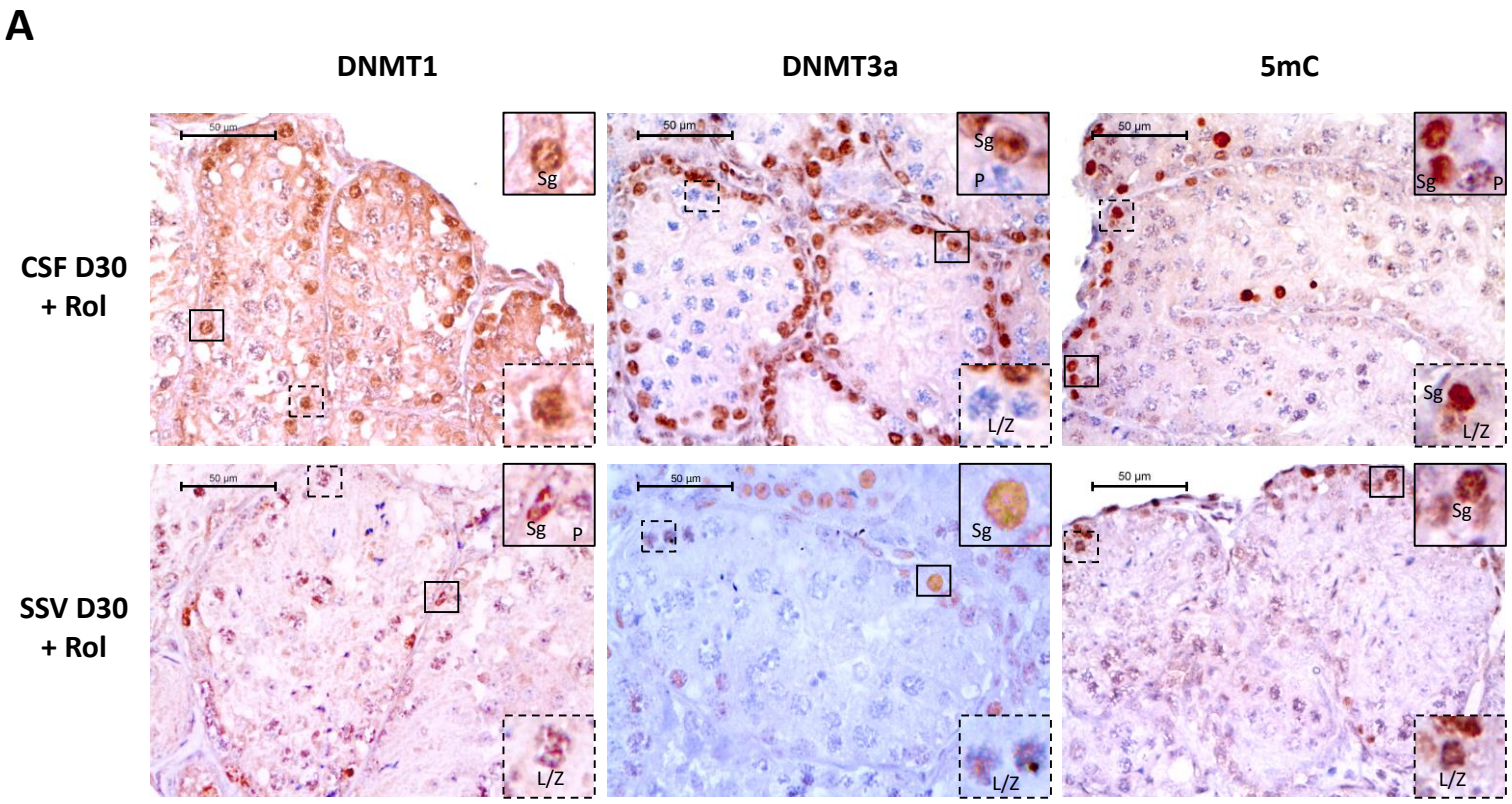
A
DNMT1
DNMT3a
5mC
CSF D30 + Rol
SSV D30 + Rol
50 µm
Sg
P
L/Z

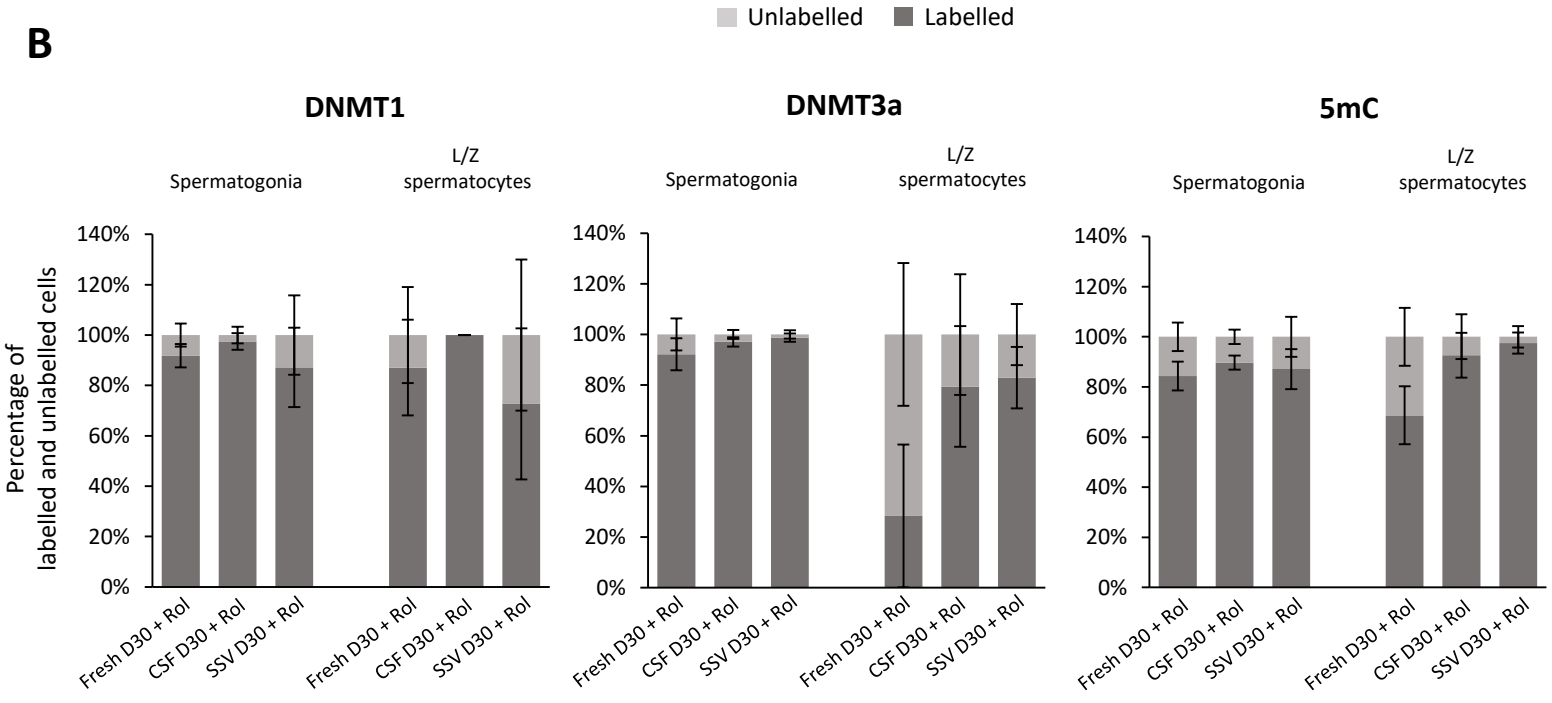
B
Unlabelled
Labelled
DNMT1
DNMT3a
5mC
Spermatogonia
L/Z spermatocytes
Percentage of labelled and unlabelled cells
140%
120%
100%
80%
60%
40%
20%
0%
Fresh D30 + Rol
CSF D30 + Rol
SSV D30 + Rol

Figure 6

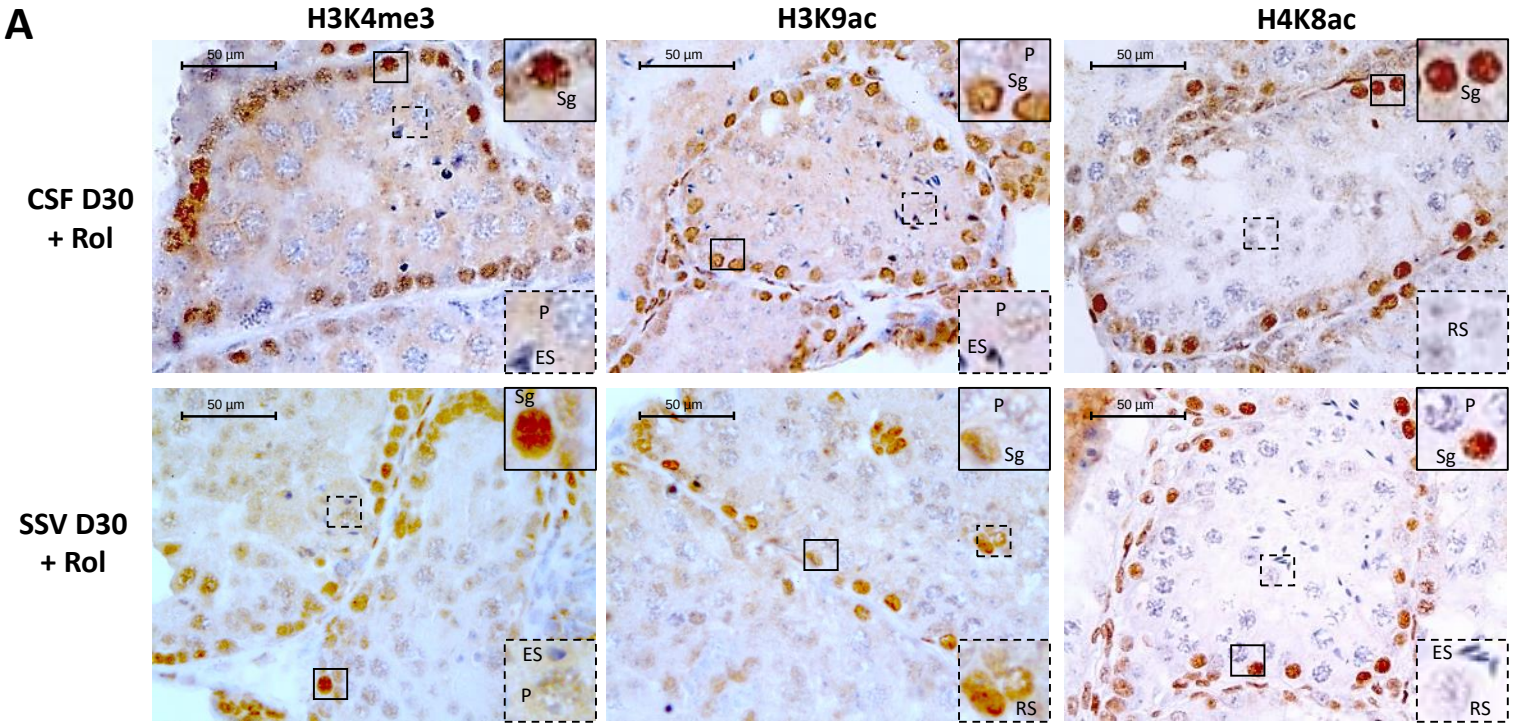
A
H3K4me3
H3K9ac
H4K8ac
CSF D30 + Rol
SSV D30 + Rol
50 µm
Sg
P
ES
RS

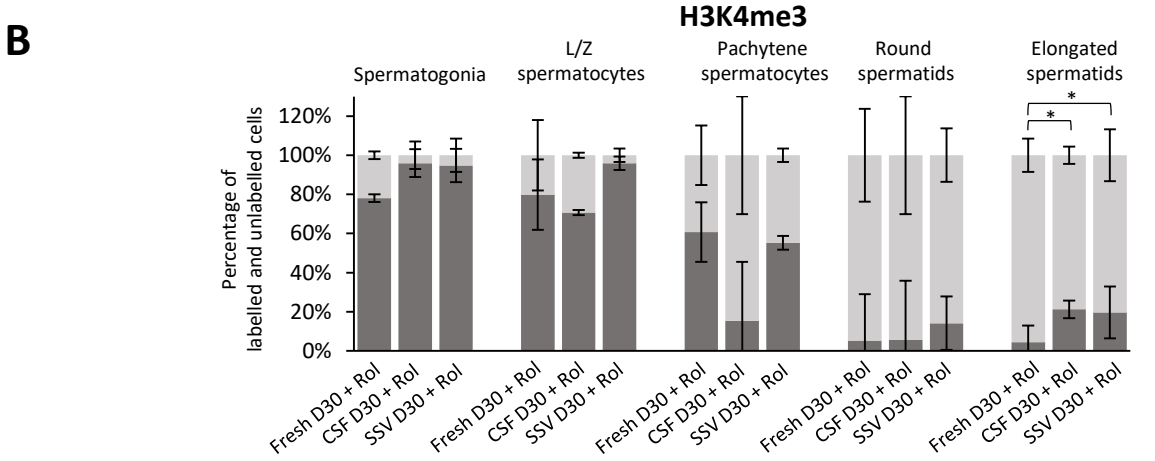
B
H3K4me3
Spermatogonia
L/Z spermatocytes
Pachytene spermatocytes
Round spermatids
Elongated spermatids
Percentage of labelled and unlabelled cells
120%
100%
80%
60%
40%
20%
0%
Fresh D30 + Rol
CSF D30 + Rol
SSV D30 + Rol

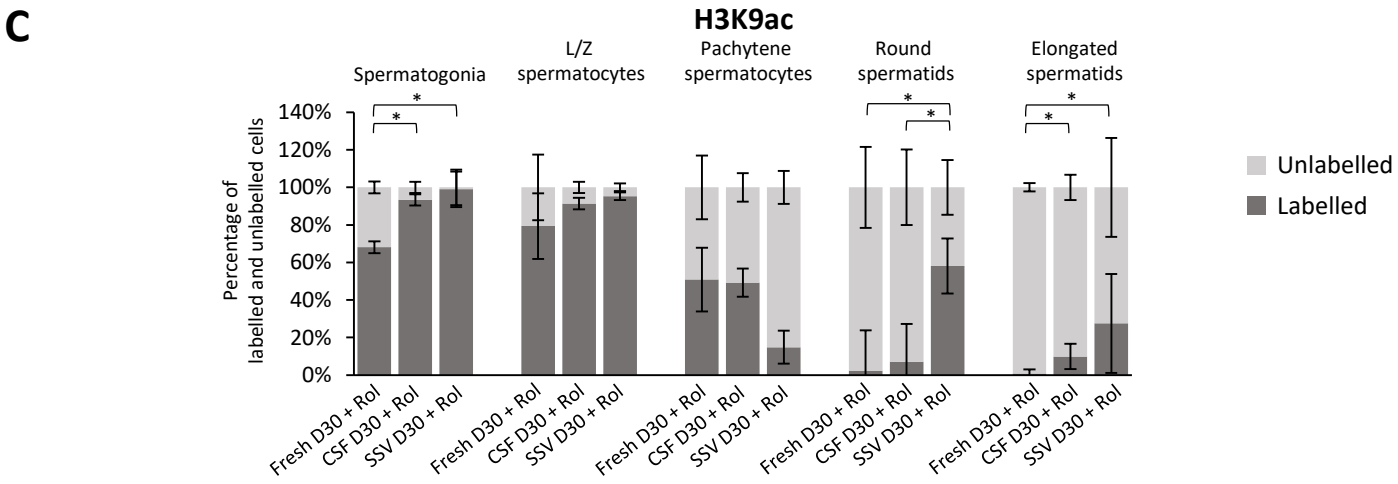
C
H3K9ac
Spermatogonia
L/Z spermatocytes
Pachytene spermatocytes
Round spermatids
Elongated spermatids
Percentage of labelled and unlabelled cells
140%
120%
100%
80%
60%
40%
20%
0%
Fresh D30 + Rol
CSF D30 + Rol
SSV D30 + Rol
Unlabelled
Labelled

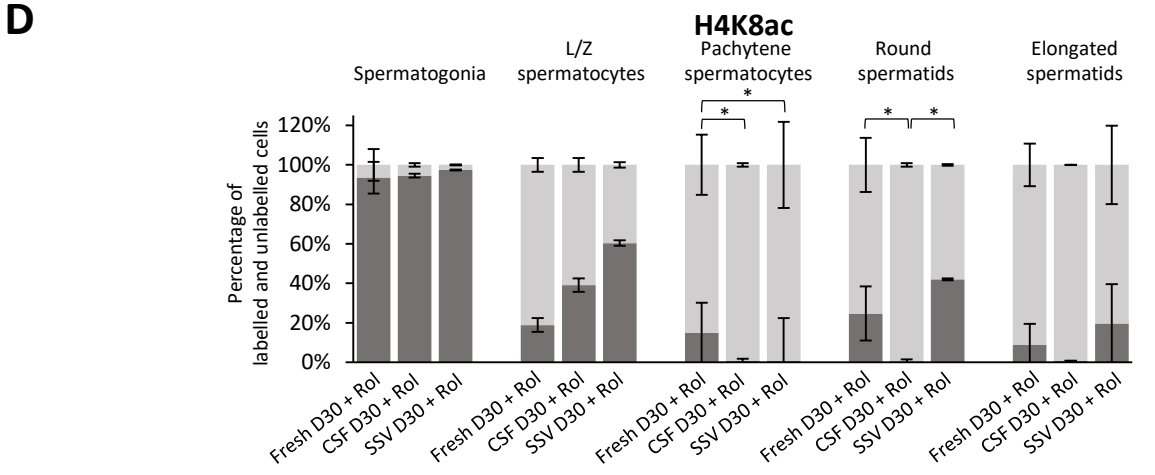
D
H4K8ac
Spermatogonia
L/Z spermatocytes
Pachytene spermatocytes
Round spermatids
Elongated spermatids
Percentage of labelled and unlabelled cells
120%
100%
80%
60%
40%
20%
0%
Fresh D30 + Rol
CSF D30 + Rol
SSV D30 + Rol

Figure 7

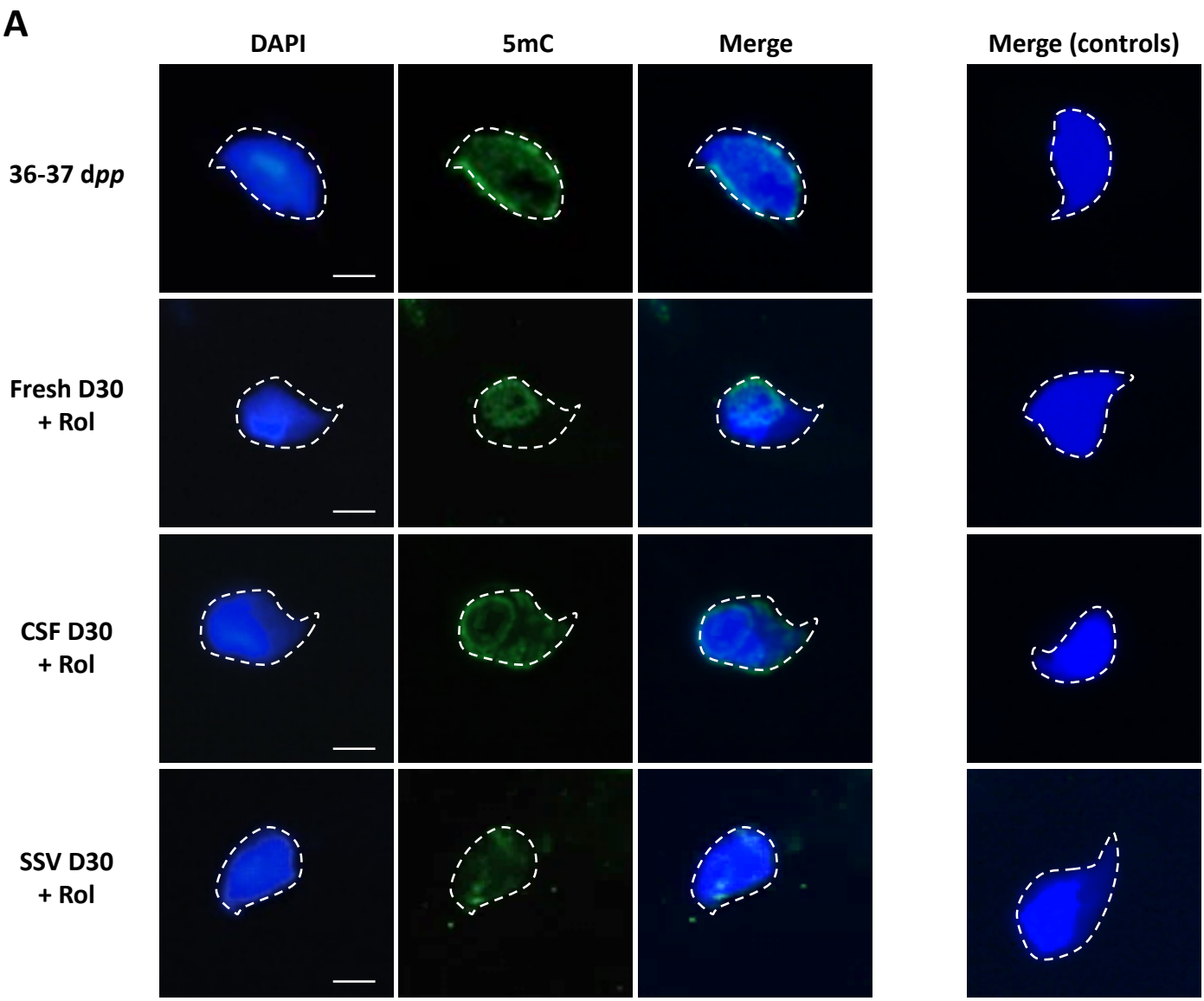
A
DAPI
5mC
Merge
Merge (controls)
36-37 dpp
Fresh D30 + Rol
CSF D30 + Rol
SSV D30 + Rol
B
**
Normalized 5mC fluorescence intensity
0
0.2
0.4
0.6
0.8
36-37 dpp
Fresh D30 + Rol
CSF D30 + Rol
SSV D30 + Rol

Table 1. Assessment of germ cell differentiation in seminiferous tubules

	% of cell types present in seminiferous tubules sections						
	36-37 d*pp*	Fresh + Rol D30	Fresh + Rol/FSH D30	CSF + Rol D30	CSF + Rol/FSH D30	SSV + Rol D30	SSV + Rol/FSH D30
Sertoli cells	9.11 (2.43)	33.13 (2.50)[a]	29.64 (5.96)[a]	39.17 (4.44)[b]	37.33 (4.78)[c]	33.59 (6.14)[d]	29.38 (5.90)[e]
Spermatogonia	7.89 (1.53)	14.78 (4.61)[a]	14.45 (3.31)[a]	20.12 (4.49)[b]	19.18 (1.92)[c]	15.94 (4.04)	15.65 (4.49)[e]
Leptotene/zygotene spermatocytes	3.24 (1.64)	4.91 (5.39)	11.91 (5.63)[a,b]	3.20 (1.53)	9.28 (4.28)[d]	3.34 (1.85)	5.69 (4.50)[f]
Pachytene spermatocytes	24.40 (2.97)	22.50 (6.12)[a]	21.63 (3.86)[a]	26.85 (5.60)	27.06 (6.25)[c]	27.42 (4.64)	32.90 (4.27)[c]
Round spermatids	37.70 (2.55)	15.15 (1.95)[a]	15.13 (5.34)[a]	7.31 (3.75)[b]	5.18 (2.60)[c]	13.83 (4.75)[d]	11.83 (3.70)[e]
Elongated spermatids	17.66 (4.32)	9.53 (3.06)[a]	7.24 (3.27)[a.b]	3.35 (1.05)[b]	1.97 (1.50)[c.d]	5.88 (2.20)	4.55 (2.53)[e]

Data are presented as the mean (SD) with n = 4 for 36-37 d*pp*, Fresh + Rol D30, Fresh + Rol/FSH D30, CSF + Rol D30, CSF + Rol/FSH D30, SSV + Rol D30, SSV + Rol/FSH D30. CSF, controlled slow freezing; D30, 30-day tissue culture; d*pp*, days *postpartum*; Rol, retinol; Rol/FSH, retinol/follicle stimulating hormone; SSV, solid surface vitrification.

[a]Values significantly different with 36-37 d*pp* ($P < 0.05$)

[b]Values significantly different with Fresh + Rol D30 ($P < 0.05$)

[c]Values significantly different with Fresh + Rol/FSH D30 ($P < 0.05$)

[d]Values significantly different with CSF + Rol D30 ($P < 0.05$)

[e]Values significantly different with CSF + Rol/FSH D30 ($P < 0.05$)

[f]Values significantly different with SSV + Rol D30 ($P < 0.05$)

Table 2. Percentage of seminiferous tubules containing differentiated germ cells at the most advanced stage

	% of seminiferous tubules at the most advanced stage						
	36-37 d*pp*	Fresh + Rol D30	Fresh + Rol/FSH D30	CSF + Rol D30	CSF + Rol/FSH D30	SSV + Rol D30	SSV + Rol/FSH D30
Spermatogonia	0	0.28 (0.96)	2.05 (2.72)[a]	3.15 (5.90)	6.17 (8.03)	3.33 (5.50)	6.13 (7.85)
Leptotene/zygotene spermatocytes	0	0.28 (0.96)	5.13 (5.89)[a.b]	0	6.94 (6.12)[d]	1.94 (4.13)	2.73 (2.29)
Pachytene spermatocytes	0	16.75 (5.08)[a]	27.64 (8.59)[a.b]	50.88 (10.82)[b]	55.37 (11.87)[c]	30.56 (15.10)[d]	47.11 (15.46)[c.e]
Round spermatids	4.72 (3.76)	33.45 (11.76)[a]	29.07 (9.46)[a]	23.33 (9.64)	18.12 (10.61)	31.11 (9.57)	17.67 (3.43)[c.e]
Elongated spermatids	95.28 (3.61)	49.24 (10.86)[a]	36.11 (10.76)[a.b]	22.64 (5.92)[b]	13.40 (7.60)[c.d]	33.06 (11.41)[b]	26.36 (14.89)

Data are presented as the mean (SD) with n = 4 for 36-37 d*pp*, Fresh + Rol D30, Fresh + Rol/FSH D30, CSF + Rol D30, CSF + Rol/FSH D30, SSV + Rol D30, SSV + Rol/FSH D30. CSF, controlled slow freezing; D30, 30-day tissue culture; d*pp*, days *postpartum*; Rol, retinol; Rol/FSH, retinol/follicle stimulating hormone; SSV, solid surface vitrification.

[a]Values significantly different with 36-37 d*pp* ($P < 0.05$)

[b]Values significantly different with Fresh + Rol D30 ($P < 0.05$)

[c]Values significantly different with Fresh + Rol/FSH D30 ($P < 0.05$)

[d]Values significantly different with CSF + Rol D30 ($P < 0.05$)

[e]Values significantly different with SSV + Rol D30 ($P < 0.05$)